

# Characterization of naturally-occurring particles in the NASA Langley 0.3-m Transonic Cryogenic Tunnel using PTV

Ross Burns, Jian Gao, and Paul Danehy (Presenter)  
ViGYAN, Inc.

The NASA Langley Research Center

AIAA SciTech 2024

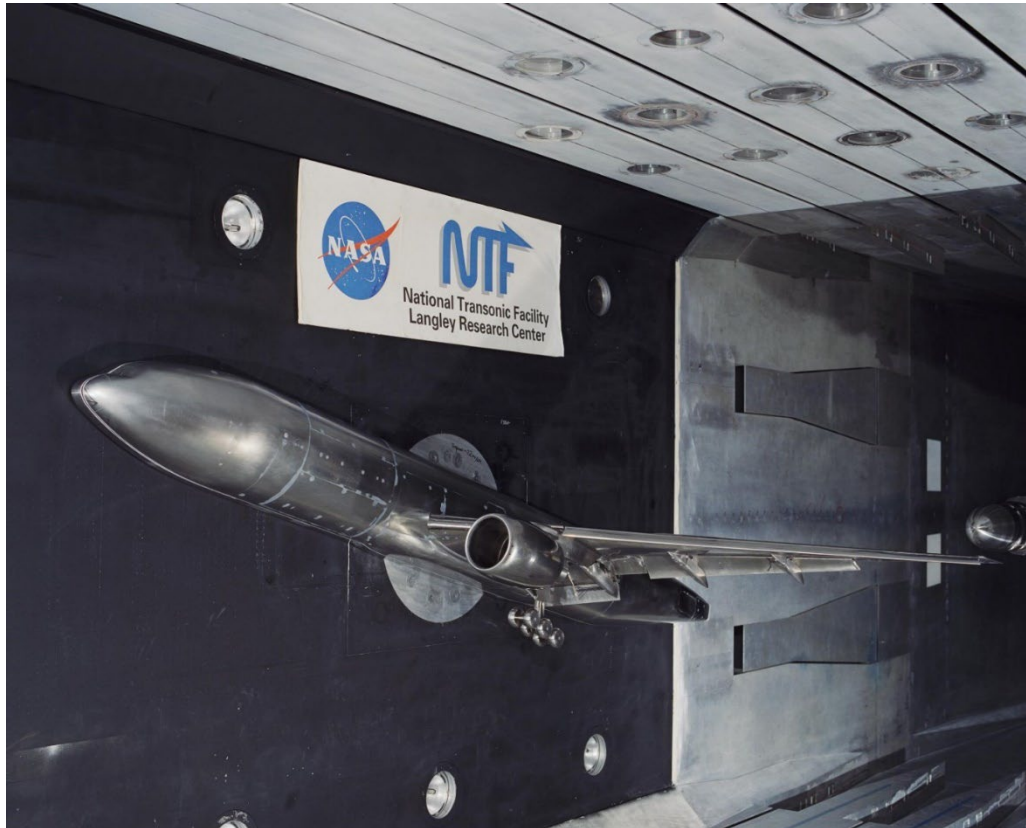
Jan 8-12, 2024



# Background and motivation

High Reynolds number testing performed in NASA Langley's Transonic Cryogenic Tunnels (TCTs)

- Flight-accurate Reynolds numbers in ground-test facilities
- Typically operate in cryogenic, pure N<sub>2</sub> environments



National Transonic Facility (NTF)  
The NASA Langley Research Center

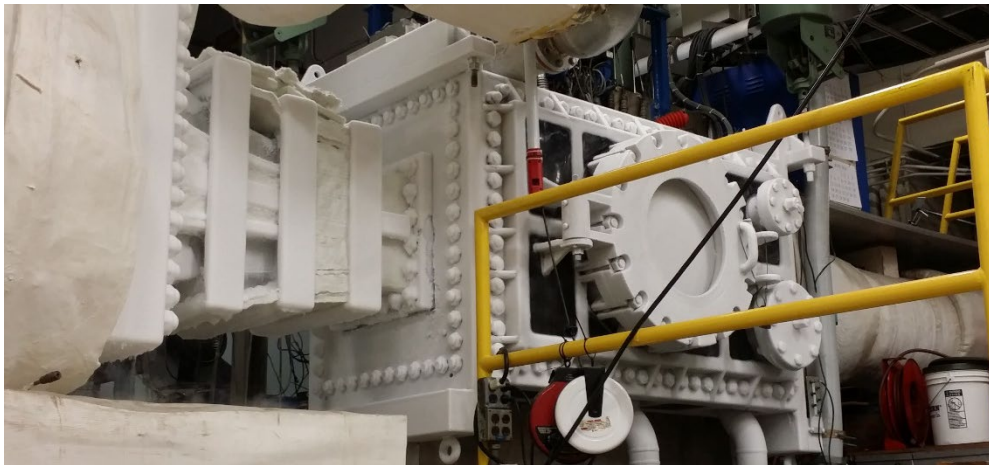
# Background and motivation

## High Reynolds number testing performed in NASA Langley's Transonic Cryogenic Tunnels (TCTs)

- Flight-accurate Reynolds numbers in ground-test facilities
- Typically operate in cryogenic, pure N<sub>2</sub> environments

## Harsh environments for experimentation

- High operating pressures and low temperatures require rugged construction
- High dynamic pressures
- Limited optical access
- Vibrations and mobile test sections
- Condensation of water and trace gases in and around facilities

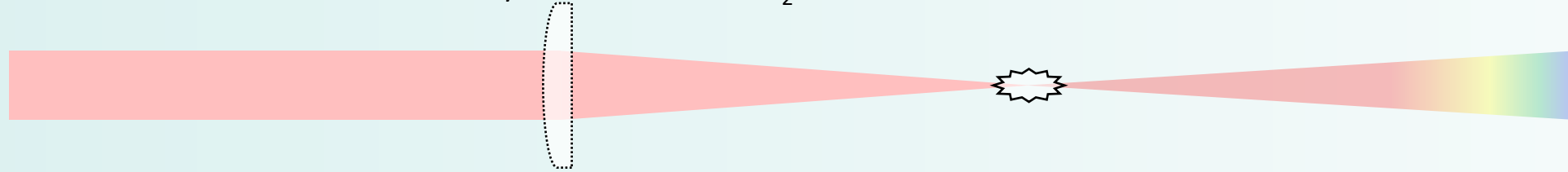


NASA Langley 0.3-m TCT frozen over after cryogenic operation

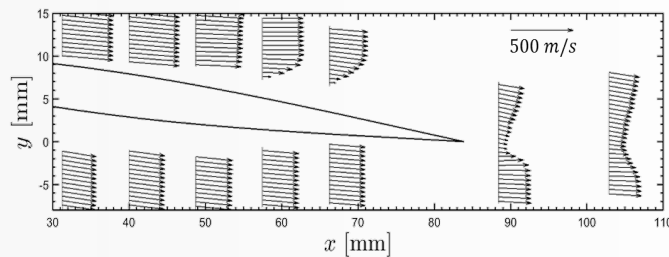
# Background and motivation

Successfully implemented a velocimetry system in NASA LaRCs TCT facilities (NTF, 0.3-m TCT) utilizing FLEET (Femtosecond Laser Electronic Excitation Tagging) velocimetry (Princeton)

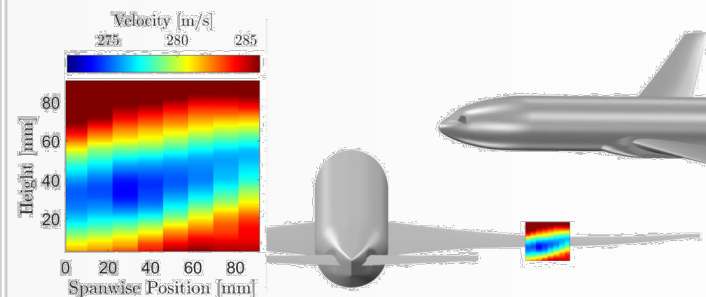
- Unseeded optical velocimetry technique
- Femtosecond laser focused to dissociate/ionize molecular  $N_2$



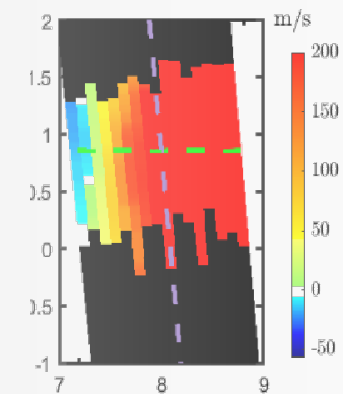
0.3-m TCT – Transonic Airfoil  
(2016)



NTF – CRM Wake Velocity  
(2018)



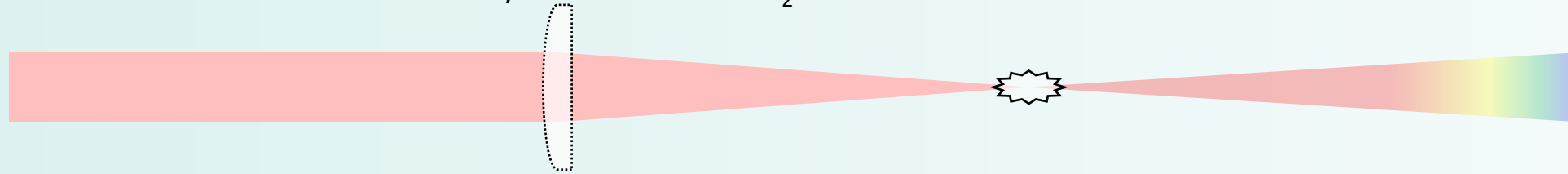
NTF – Orion Crew Capsule  
(2022)



# Background and motivation

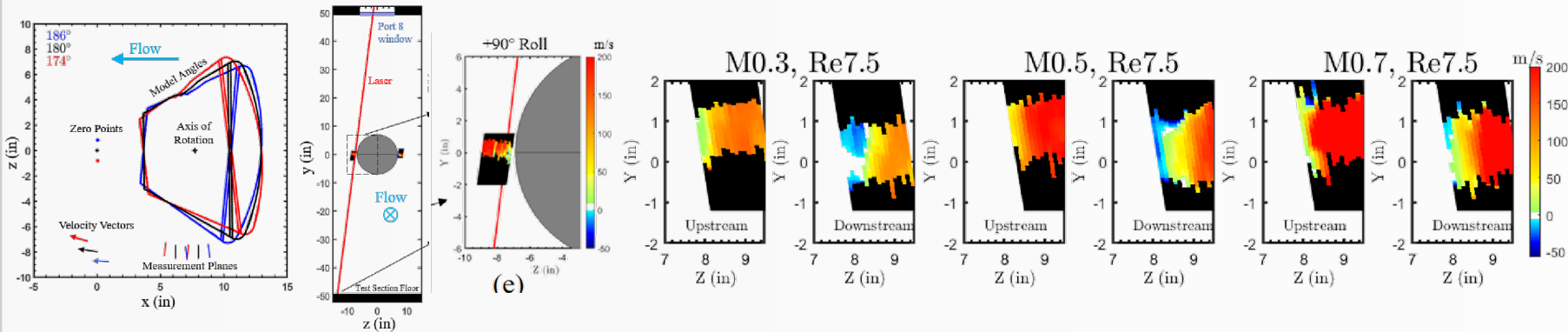
Successfully implemented a velocimetry system in NASA LaRCs TCT facilities (NTF, 0.3-m TCT) utilizing FLEET (Femtosecond Laser Electronic Excitation Tagging) velocimetry (Princeton)

- Unseeded optical velocimetry technique
- Femtosecond laser focused to dissociate/ionize molecular  $N_2$



## NTF – Orion Crew Capsule (2022)

- Measured two-dimensional planes of velocity in the wake of a scale Orion model



### Single-Component Average Velocity Profiles in the Wake of the Orion Crew Capsule at the National Transonic Facility

Jonathan E. Retter<sup>1</sup> and Olivia Tyrrell<sup>2</sup>  
National Institute of Aerospace, Hampton, VA, 23666, United States

Bryce Moran<sup>3</sup>, James Montgomery<sup>4</sup>, and Bill Dressler<sup>5</sup>  
Jacobs Technology, Inc., Hampton, VA, 23666, United States

Karen L. Bibb<sup>6</sup>, Gregory J. Brauckmann<sup>7</sup>, Daniel T. Reese<sup>8</sup> and Paul M. Danehy<sup>9</sup>

NASA Langley Research Center, Hampton, VA, 23681, United States

A minimally intrusive molecular tagging instrument measured single-component average velocity profiles in two planes in the wake of the Orion capsule with different heat shield configurations in the National Transonic Facility at the NASA Langley Research Center. Reynolds number effects at subsonic conditions have proven difficult to predict due to the largely separated wake flow. Therefore two measurement planes in the wake of the model were probed to measure the wake profile for different heat shield configurations and act as a validation reference for computational tools. Air testing included Mach numbers of 0.3, 0.5, and 0.7 at Reynolds numbers of 5.3 and 7.5 million. In cryogenic nitrogen, the instrument was employed under transient conditions during the facility warm up at  $M = 0.3$  with decreasing Reynolds numbers from 16 million. An exhaustive list of the results is shown and discussed here. For free transition heat shield configurations, the size of the wake was found to increase with Mach number, yet remain constant with Reynolds number for low ( $M = 0.3$ ) and high ( $M = 0.7$ ) subsonic Mach numbers. However, intermediate Mach numbers ( $M = 0.5$ ) showed that the wake was smaller at higher Reynolds numbers for the IDAT heat shield. The addition of surface roughness in the form of grit, known as the fixed transition cases, negated any Mach number dependence to the wake profile and increased the size of the wake for all cases.

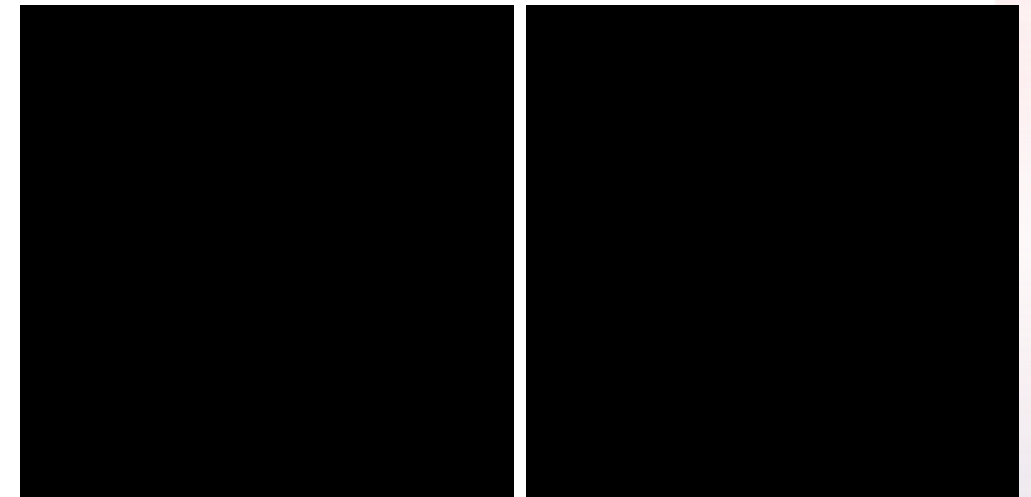
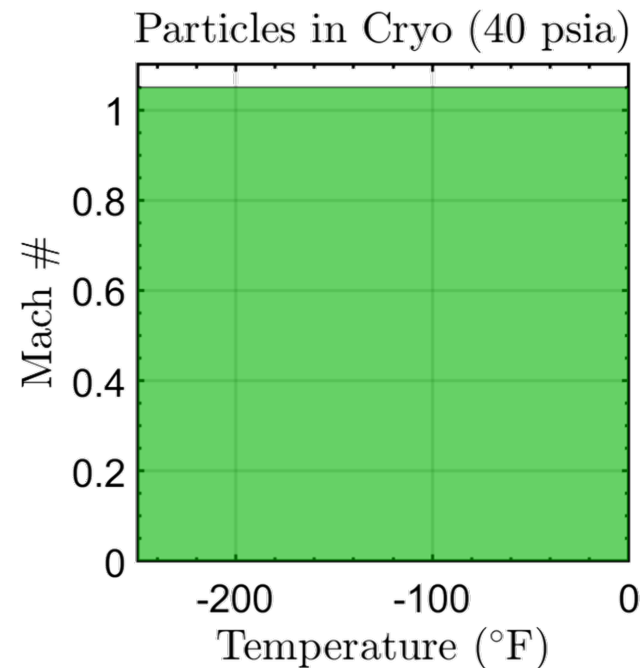
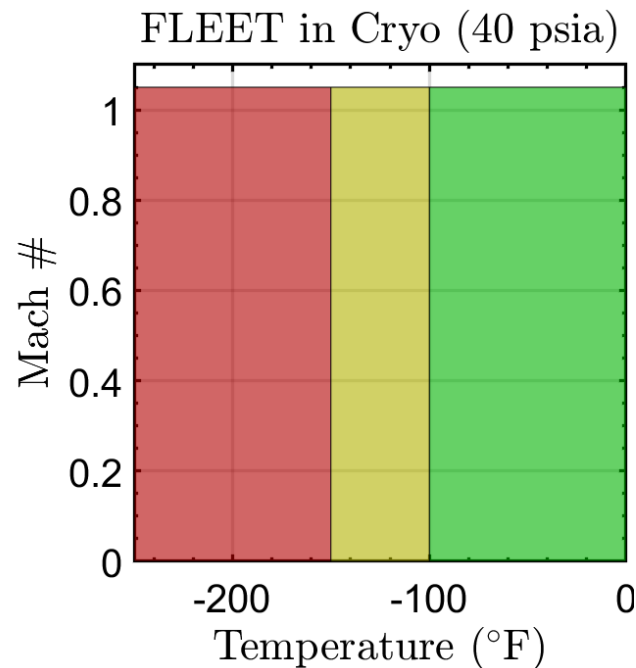
Retter, JE, Tyrrell, O, Moran, B, Montgomery, J, Dressler, B, Bibb, KL, Brauckmann, GJ, Reese, DT, and Danehy, PM, "Single-Component Average Velocity Profiles in the Wake of the Orion Crew Capsule at the National Transonic Facility," AIAA SciTech 2023

# Background and motivation

## Transition to particle-based measurements

- While the implementation of FLEET was successful in certain flow regimes at the NTF, to date FLEET has not been successful during the highest-Reynolds-number part of the operational envelope
  - Practical limitations of LPS and measurement geometry
- Naturally-occurring particles have been observed over most of the operational envelope in both NASA LaRC TCT facilities
  - Detailed by Herring *et al.* NASA/TM-2015-218800
- Since artificial seeding is a nonstarter in the NTF, **need to characterize the aerodynamic behavior of the naturally occurring particles before they can be utilized for diagnostics**

Particles in warm Air (dust?), cool and cold  $N_2$ . (water ice\*,  $LN_2$ )



\*Qi, Y., Ye, H., and Hu, Q., "Mechanisms of trace water vapor desublimation over airfoil in transonic cryogenic wind tunnels," *Physics of Fluids*, Vol. 34, 2022.

# Test Objectives for Current Work at 0.3 m TCT

Establish and test a framework by which naturally-occurring particles can be assessed *in situ* for their aerodynamic performance

- Tests were carried out in the NASA LaRC 0.3-m TCT (pilot facility for NTF)
  - Particles are known to be present over most of the operational envelope in this facility as well
- Test was divided into two phases
  - **Phase 1:** assess particle aerodynamic response across a normal shockwave (***How big are the particles?***)
  - **Phase 2:** observe practical behavior of particles under high-lift operating conditions (sensitivity to flow separation) (***Will the particles track the separated flow?***)

# Experimental Setup

---

# Experimental Setup

## The NASA Langley 0.3-m Transonic Cryogenic Tunnel (0.3-m TCT)

- Continuous, closed-circuit wind tunnel operating with air or  $N_2$
- Mach number range: 0.2 to 0.9
- Total pressure range: 100 kPa to 500 kPa
- Total temperature range: 95 K to 320 K
- Double-shelled construction

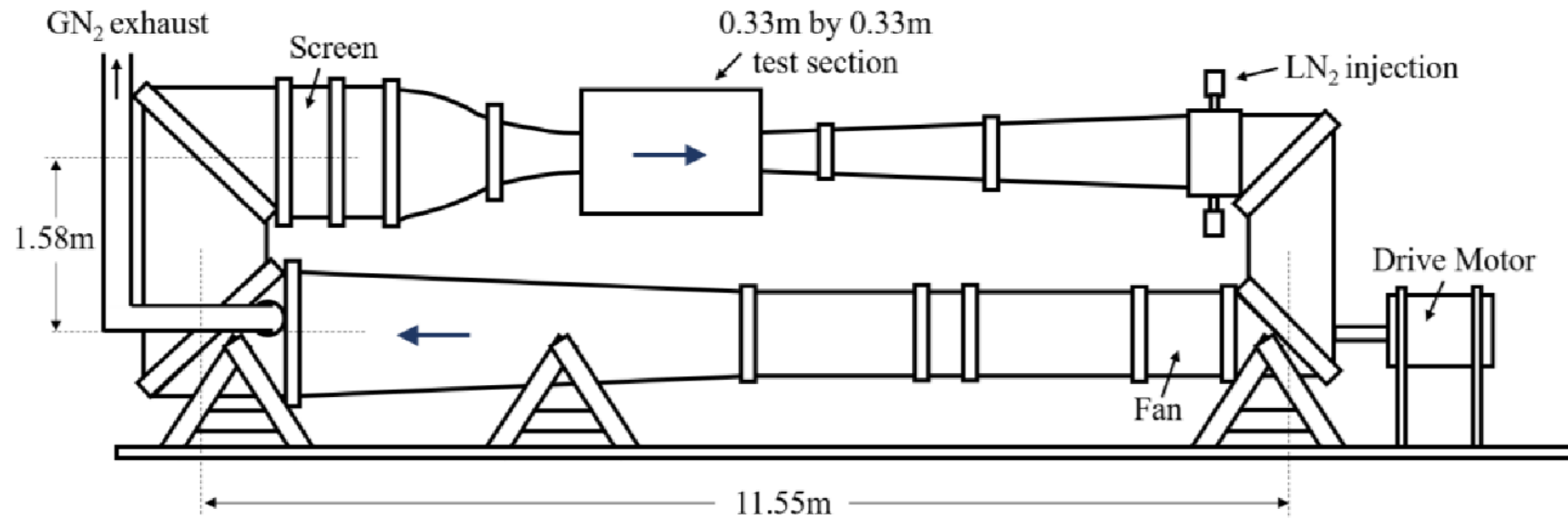
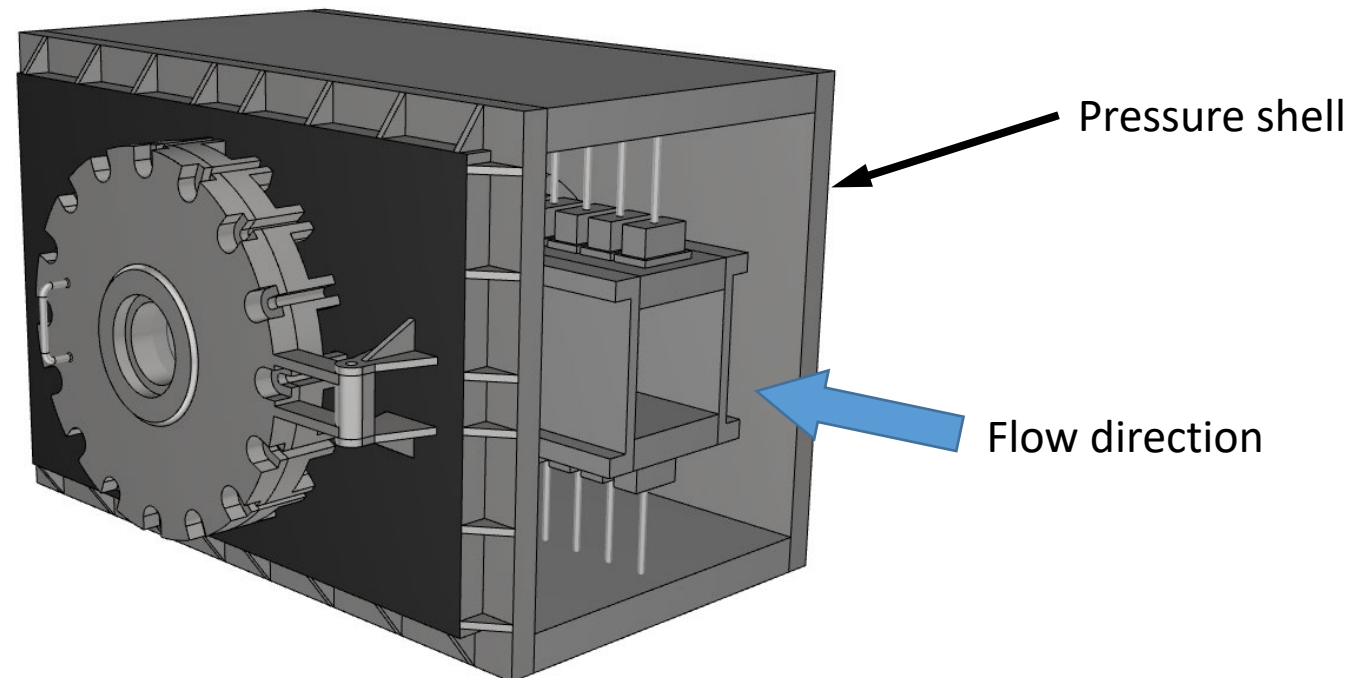


Diagram of 0.3-m TCT facility

# Experimental Setup

## The NASA Langley 0.3-m Transonic Cryogenic Tunnel (0.3-m TCT)

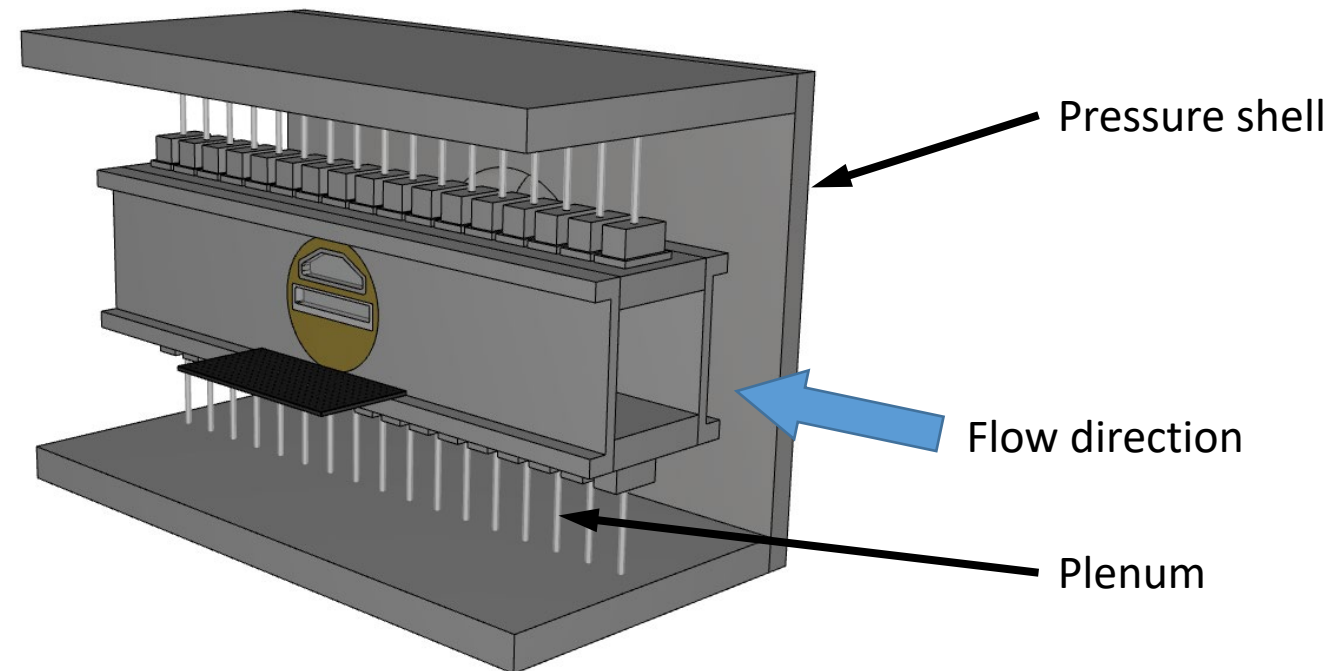
- Continuous, closed-circuit wind tunnel operating with air or  $N_2$
- Mach number range: 0.2 to 0.9
- Total pressure range: 100 kPa to 500 kPa
- Total temperature range: 95 K to 320 K
- Double-shelled construction



# Experimental Setup

## The NASA Langley 0.3-m Transonic Cryogenic Tunnel (0.3-m TCT)

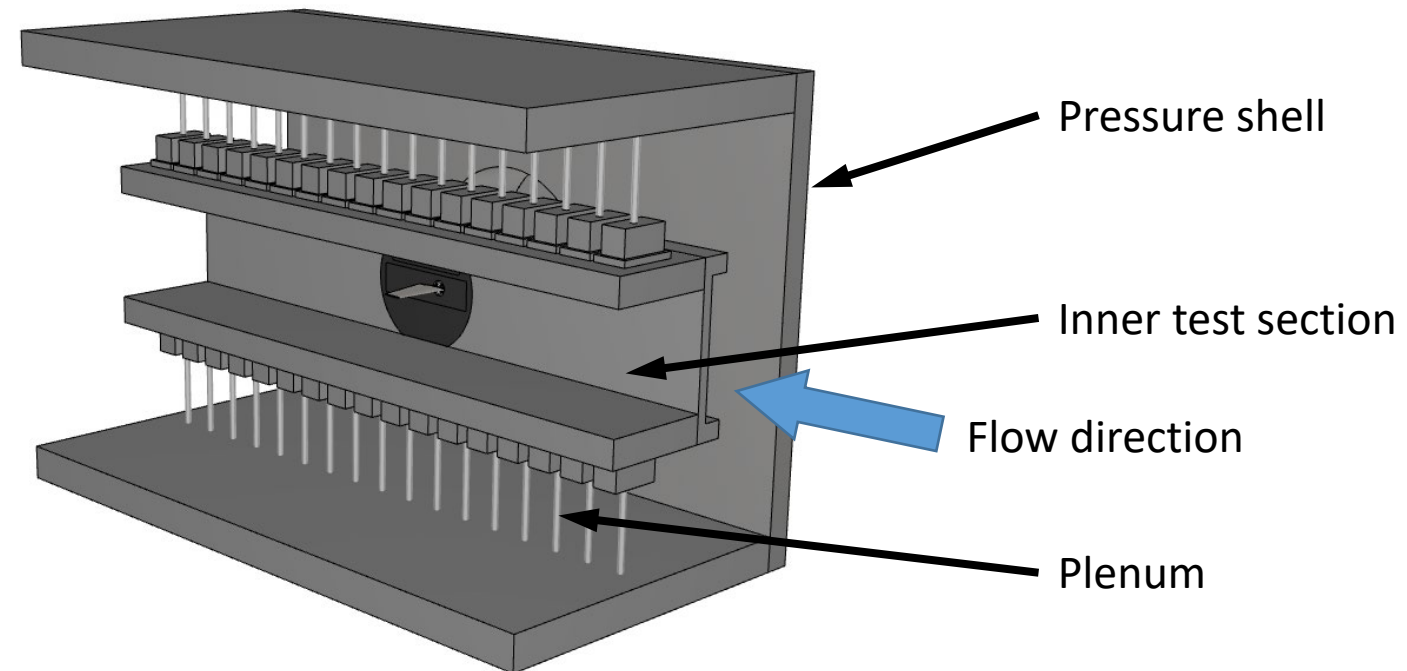
- Continuous, closed-circuit wind tunnel operating with air or N<sub>2</sub>
- Mach number range: 0.2 to 0.9
- Total pressure range: 100 kPa to 500 kPa
- Total temperature range: 95 K to 320 K
- Double-shelled construction



# Experimental Setup

## The NASA Langley 0.3-m Transonic Cryogenic Tunnel (0.3-m TCT)

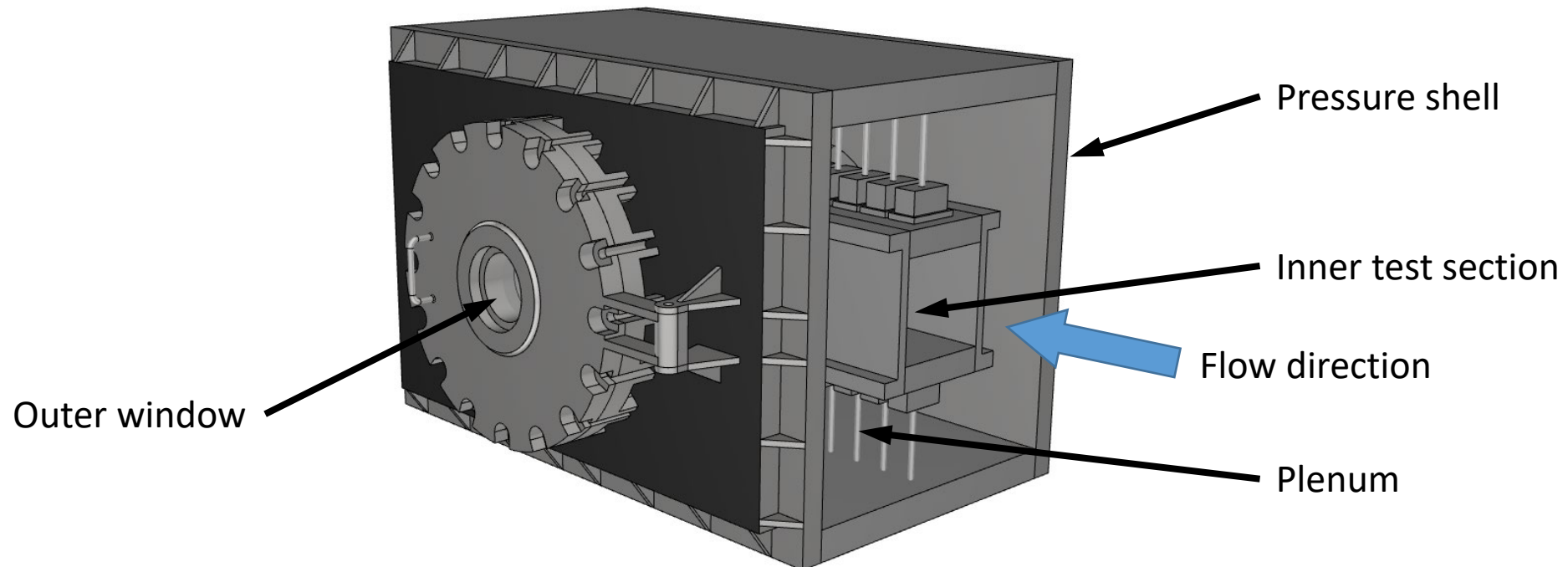
- Continuous, closed-circuit wind tunnel operating with air or  $N_2$
- Mach number range: 0.2 to 0.9
- Total pressure range: 100 kPa to 500 kPa
- Total temperature range: 95 K to 320 K
- Double-shelled construction



# Experimental Setup

## The NASA Langley 0.3-m Transonic Cryogenic Tunnel (0.3-m TCT)

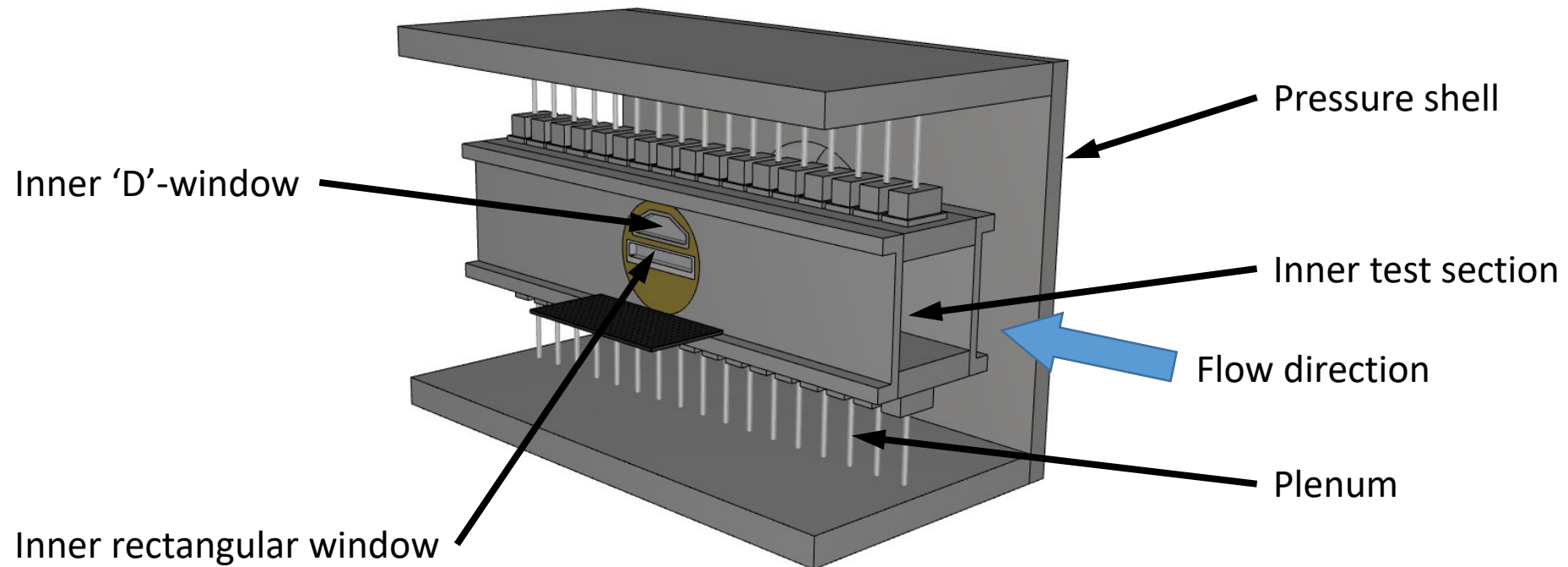
- Continuous, closed-circuit wind tunnel operating with air or  $N_2$
- Mach number range: 0.2 to 0.9
- Total pressure range: 100 kPa to 500 kPa
- Total temperature range: 95 K to 320 K
- Double-shelled construction
- Optical access: outer pressure shell window + two windows in turntable



# Experimental Setup

## The NASA Langley 0.3-m Transonic Cryogenic Tunnel (0.3-m TCT)

- Continuous, closed-circuit wind tunnel operating with air or N<sub>2</sub>
- Mach number range: 0.2 to 0.9
- Total pressure range: 100 kPa to 500 kPa
- Total temperature range: 95 K to 320 K
- Double-shelled construction
- Optical access: outer pressure shell window + two windows in turntable



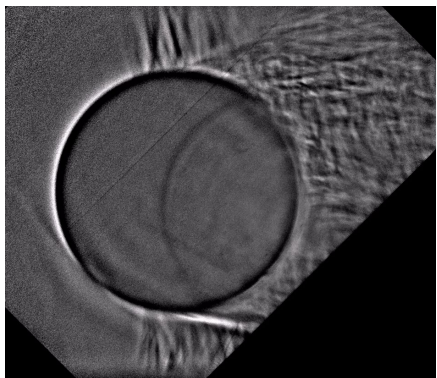
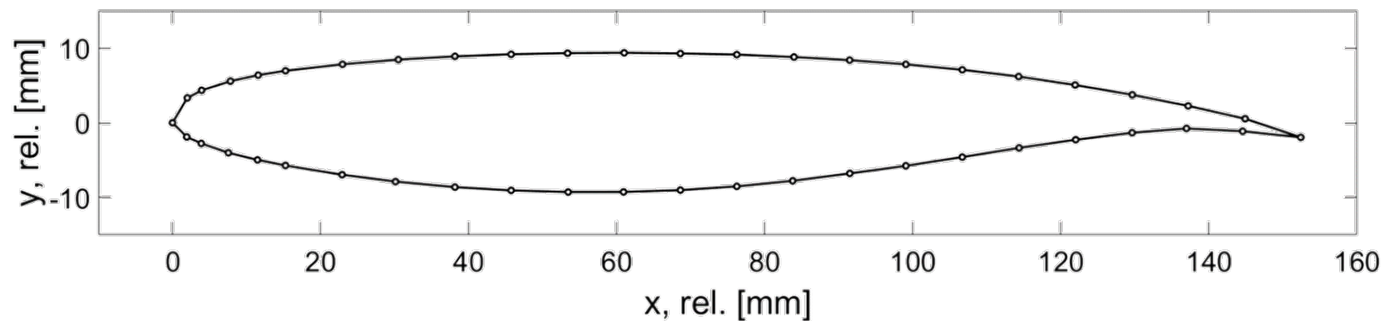
# Experimental Setup, Phase 1

---

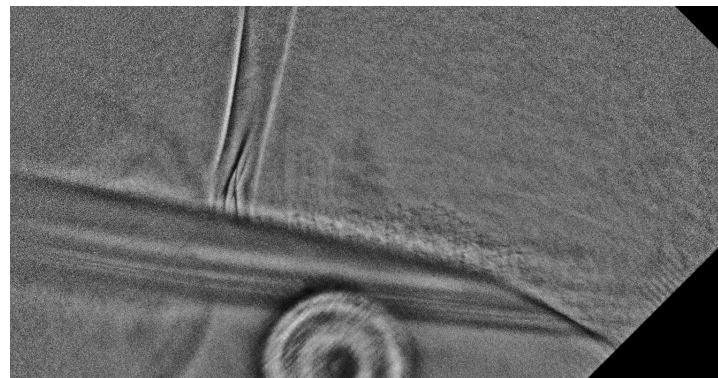
# Experimental Setup, Phase 1

**Phase 1 Studies** – Assess aerodynamic behavior of naturally-occurring particles through a normal shock

- Ultimately utilized a full-span, supercritical airfoil to generate shock
  - SC(3)-0712(B)
  - Experiments were informed by a Self-Aligned Focusing Schlieren system (Weisberger et al., companion paper Friday)
  - Full-span airfoil provided the most positionally-stable shockwave of all available and tested models



3/4-span cylinder



semi-span airfoil



full-span airfoil (10 fps)

## Self-Aligned Focusing Schlieren at the 0.3-M Transonic Cryogenic Tunnel and the National Transonic Facility

Joshua M. Weisberger\*, Brett F. Bathel<sup>†</sup>, Paul M. Danehy<sup>‡</sup>, Matthew T. Boyda<sup>§</sup>, Olivia K. Tyrrell<sup>¶</sup>, W. Holt Ripley<sup>||</sup>, and Gregory S. Jones\*\*

NASA Langley Research Center, Hampton, VA, 23681

Ross A. Burns<sup>††</sup>

ViGYAN, Inc., Hampton, VA, 23666

Andy K. Kwok<sup>‡‡</sup>

Jacobs Technology Inc., Hampton, VA, 23681

Stephen B. Jones<sup>§§</sup>

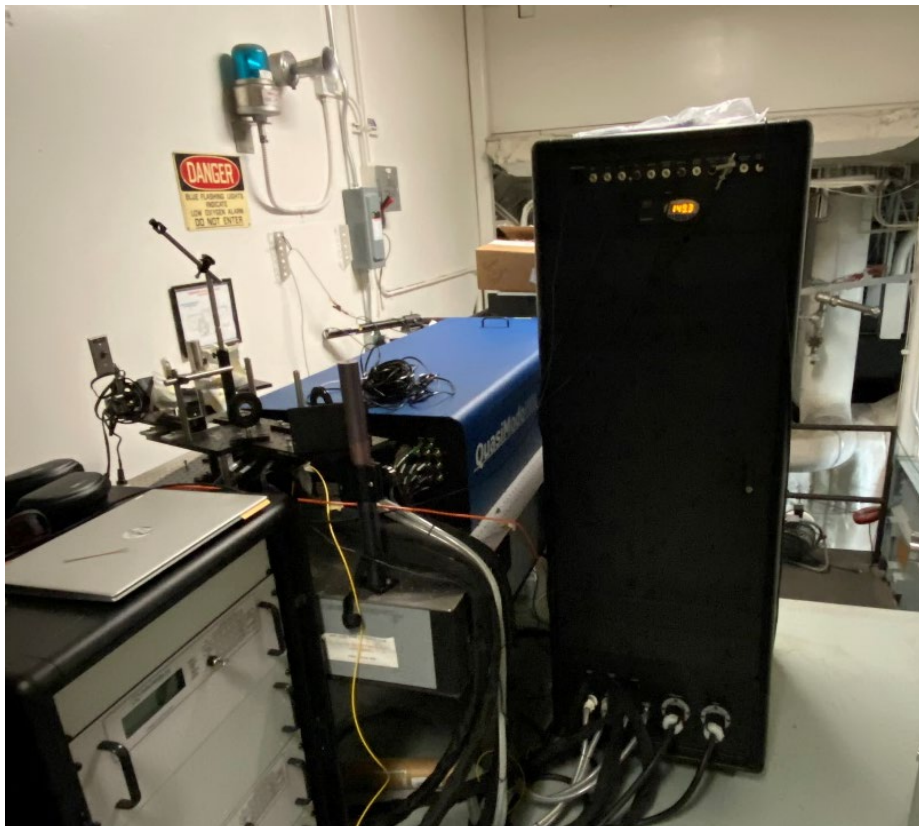
Analytical Mechanics Associates, Inc., Hampton, VA, 23681

The implementation of a self-aligned focusing schlieren (SAFS) system at two cryogenic wind tunnels at NASA Langley Research Center is discussed. Risk-reduction testing of the SAFS system was first performed at the 0.3-M Transonic Cryogenic Tunnel to evaluate the system's operation in a small-scale characteristic cryogenic facility. Testing was conducted with three models: a three-quarter span 25.4-mm-diameter cylinder, a semi-span 65A006 tapered unswept airfoil, and a full-span SC(3)-0712 airfoil. Testing with the cylinder and semi-span airfoil revealed a highly dynamic shock environment, whereas the shock on the full-span airfoil was stationary, solidifying the usage of this model for a pre-/post-shock particle tracking velocimetry measurement. Temperature-induced polarization-altering window stresses were encountered during low-temperature testing, and were mitigated using a "non-ideal" quartz/quartz Rochon prism that had largely been neglected since the SAFS system's first introduction in favor of the more favorable "ideal" glass/quartz Rochon prism. The size of the SAFS system was then decreased in order to fit inside an environmentally-controlled camera enclosure at the National Transonic Facility (NTF) for testing of a sting-mounted aircraft model. The SAFS system was demonstrated to be effective at filtering out the large density gradient flow in the 0.3-M plenum, and the thick, high density turbulent boundary layers on the wind tunnel walls at the NTF. Results of the testing campaigns and improvements to future systems are discussed.

# Experimental Setup, Phase 1

Laser and imaging systems

- Burst-mode laser

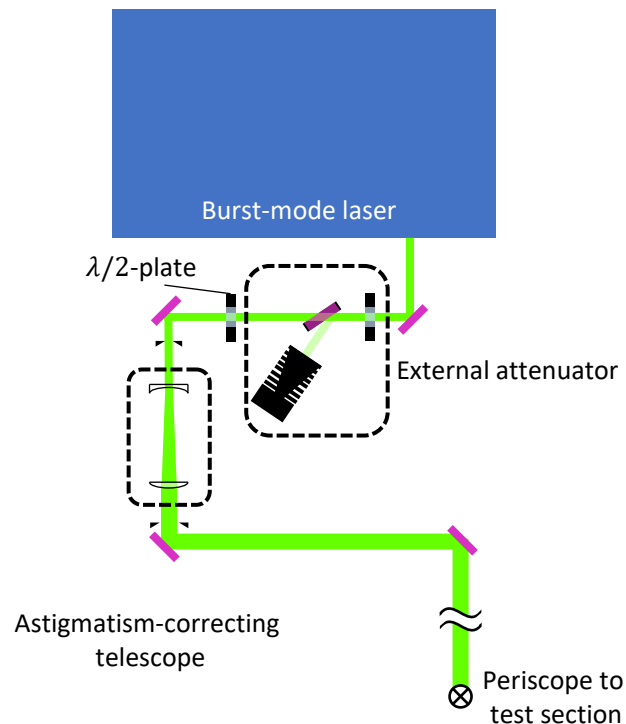


Center Wavelength	532.217 nm
Pulse Duration	20 ns
Repetition Rate	20 kHz
Operating Mode	Double pulse/ 2.5 or 5 $\mu$ s delay
Burst Duration	10 ms
Burst Period	12 s

# Experimental Setup, Phase 1

## Laser and imaging systems

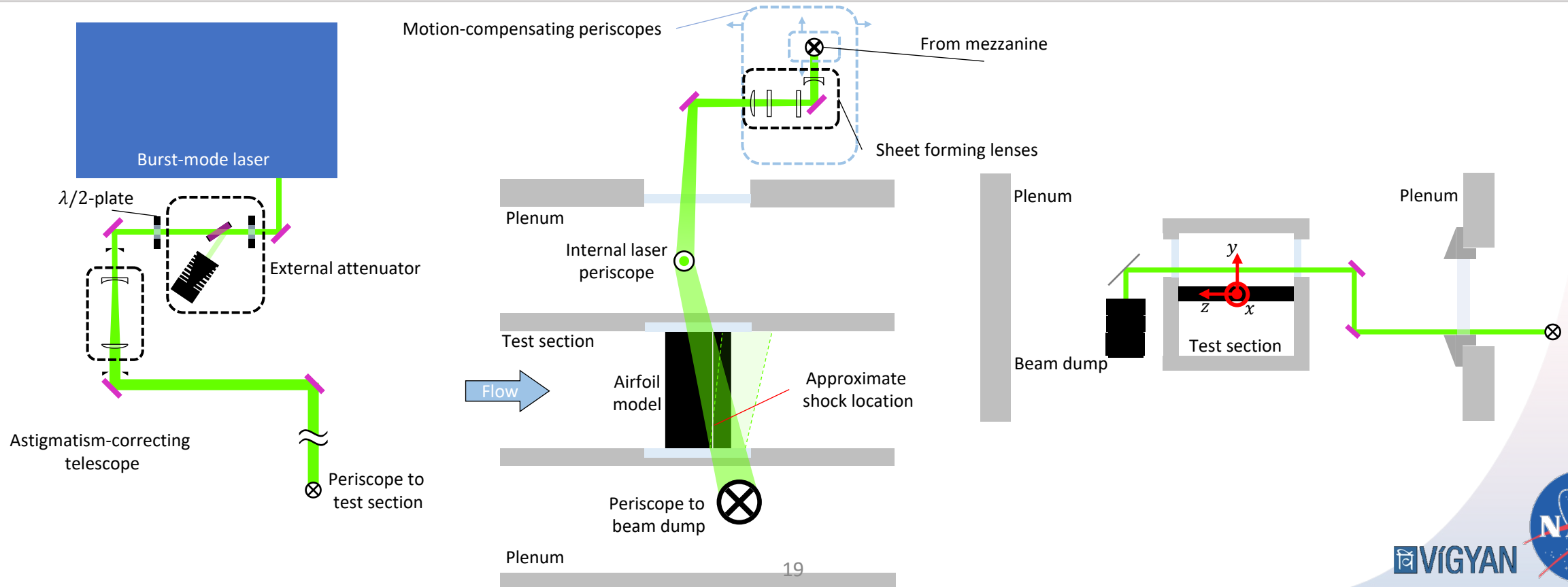
- Burst-mode laser
- Beam directed through an external attenuator and astigmatism-correcting optics before being routed to test section



# Experimental Setup, Phase 1

## Laser and imaging systems

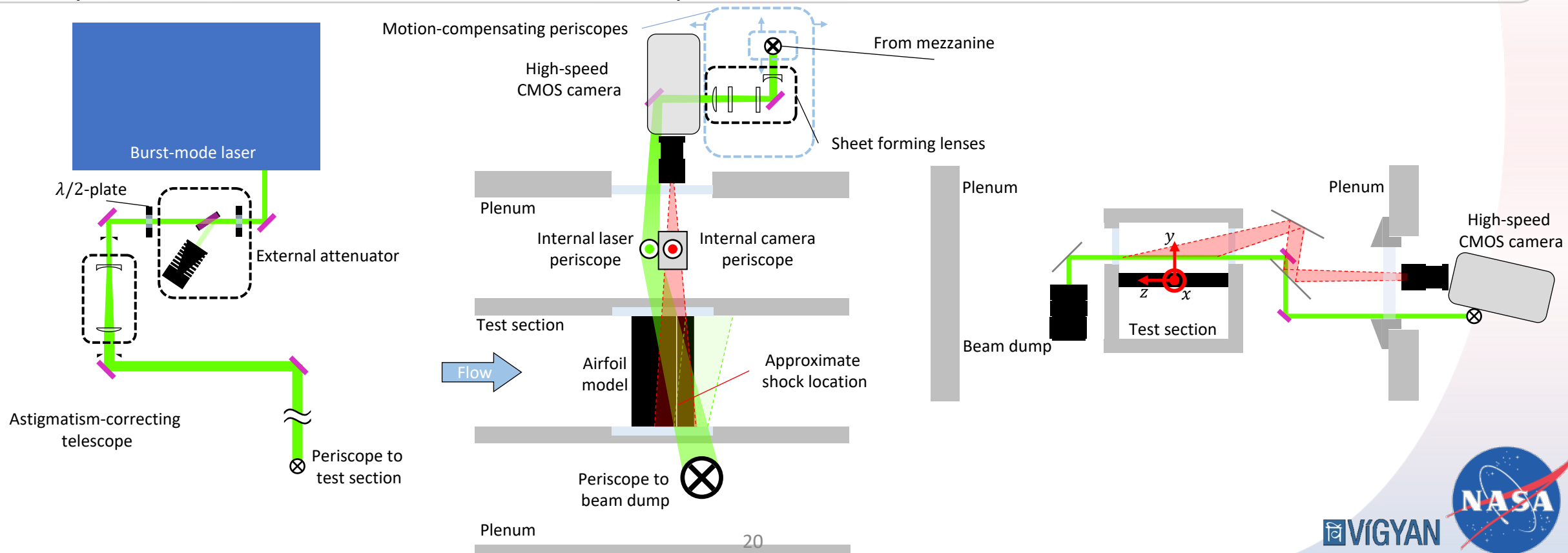
- Burst-mode laser
- Beam directed through an external attenuator and astigmatism-correcting optics before being routed to test section
- Sheet forming optics near test section and an internal beam periscope to position sheet horizontally over the surface of the airfoil



# Experimental Setup, Phase 1

## Laser and imaging systems

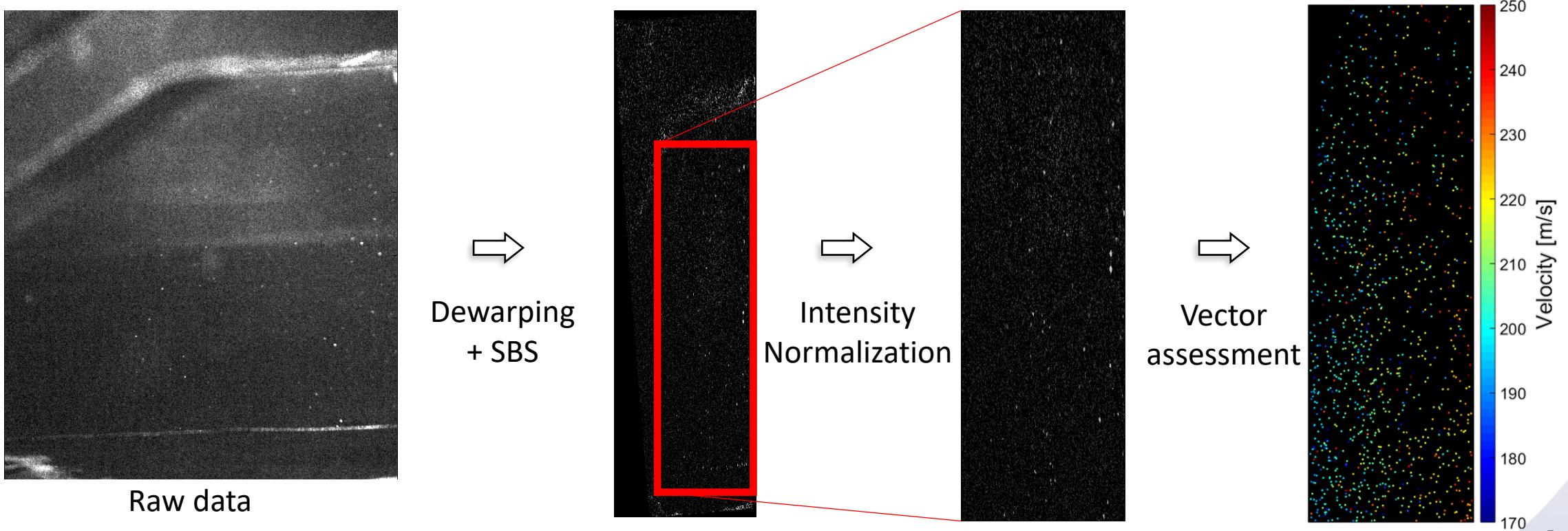
- Burst-mode laser
- Beam directed through an external attenuator and astigmatism-correcting optics before being routed to test section
- Sheet forming optics near test section and an internal beam periscope to position sheet horizontally over the surface of the airfoil
- High-speed CMOS camera viewed through same window, Scheimpflug mount and second internal periscope required
  - Operated at 40 kHz to frame-straddle the double pulse from the burst-mode laser



# Experimental Setup, Phase 1

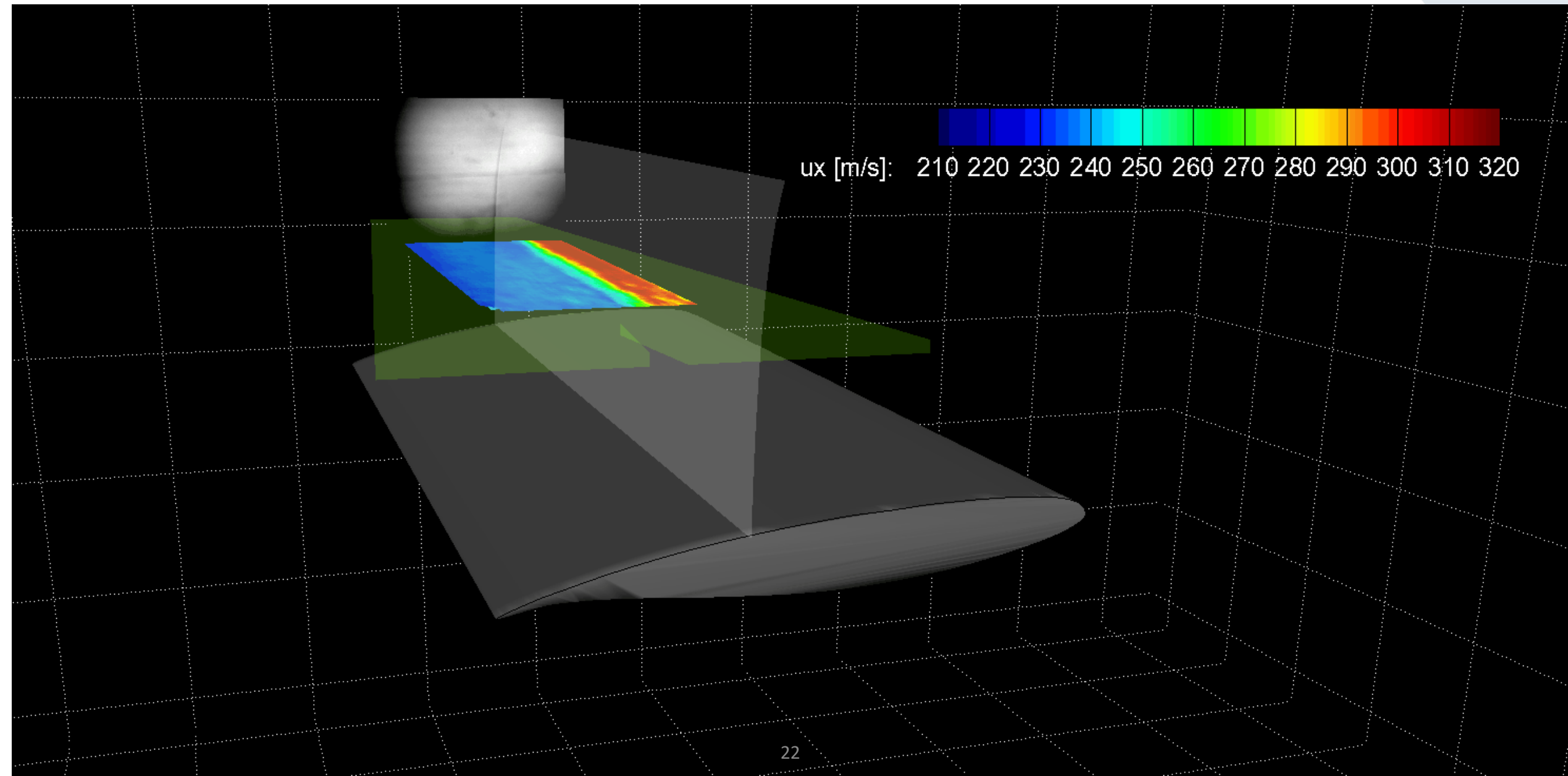
## Data Sample

- Scattering imaged through D-window (principally back-scatter, low intensity)
  - Very low SNR ( $\mathcal{O}(1)$ )
- Had to limit tunnel operating temperature to  $> 200$  K (condensation within plenum)
- Performed particle tracking velocimetry (PTV) due to the low particle flux at this elevated temperature
- Data were subjected to numerous pre- and post-processing steps to successfully identify particles and assess displacements/velocity (see paper for more details)



# Visualization of wing, schlieren, shock and velocimetry

(Flow is right to left)

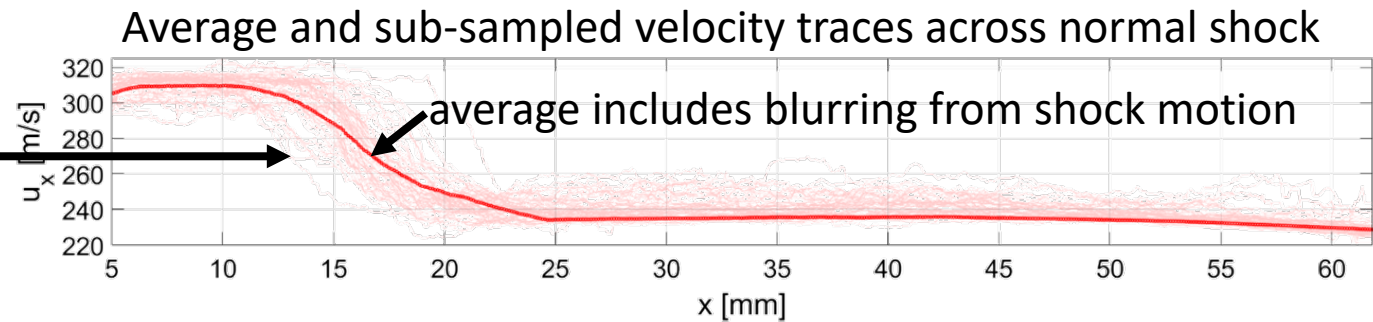
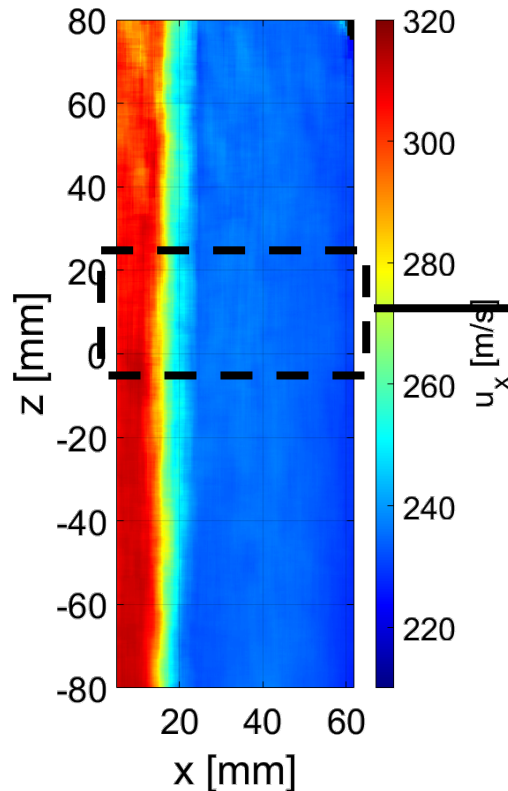


# Results, Phase 1

Primary case –  $M_\infty = 0.74$ ,  $P_t = 192$  kPa,  $T_t = 200$  K,  $\alpha = 4^\circ$

- Normal shock visible near upstream edge of measurement region
- Total shock movement detected to be  $\sim 10$  mm over all measurements (smallest of all tested cases)
- Obvious effects of particle inertia in integrated velocity traces

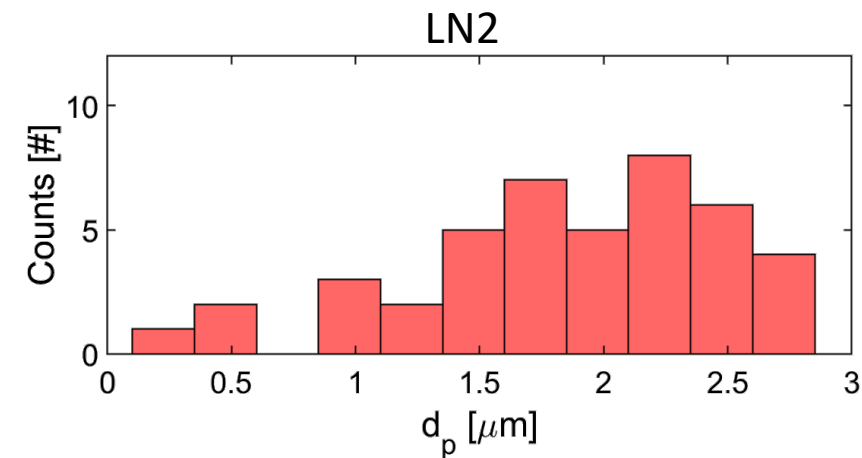
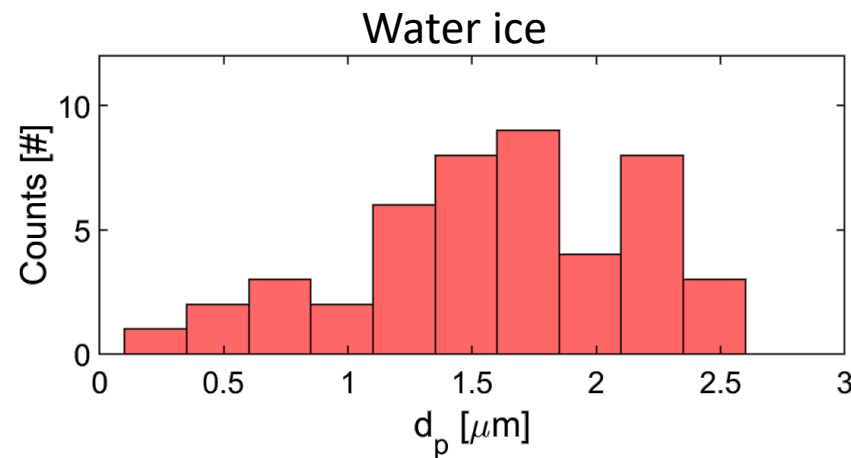
Ensemble averaged 2D velocity field



# Results, Phase 1

Primary case –  $M_\infty = 0.74$ ,  $P_t = 192$  kPa,  $T_t = 200$  K,  $\alpha = 4^\circ$

- Normal shock visible near upstream edge of measurement region
- Total shock movement detected to be  $\sim 10$  mm over all measurements (smallest of all tested cases)
- Obvious effects of particle inertia in integrated velocity traces
- Velocity traces fit for particle response using relations of Loth [1] with correction by Williams [2]
  - Composition unknown, assumed both LN2 and water ice
- **Mean particle diameter lied between 1.6 and 1.9  $\mu\text{m}$** , with the overall range between 0.2 and 3.5  $\mu\text{m}$
- Previous measurements ( $\sim 40$  years ago) by Hall et al. found the most prevalent particle diameter to be around 3  $\mu\text{m}$  with significant variance in the measurement [3]



[1] Loth, E., "Compressibility and Rarefaction Effects on Drag of a Spherical Particle," AIAA Journal, Vol. 46, No. 9, 2008.

[2] Williams, OJH, Nguyen, T., Schreyer, AM, and Smits, AJ, "Particle response analysis for particle image velocimetry in supersonic flows," Physics of Fluids, Vol. 27, 2015.

[3] Hall, RM, "Pre-Existing Seed Particles and the Onset of Condensation in Cryogenic Wind Tunnels," AIAA 22nd Aerospace Sciences Meeting, 1984.

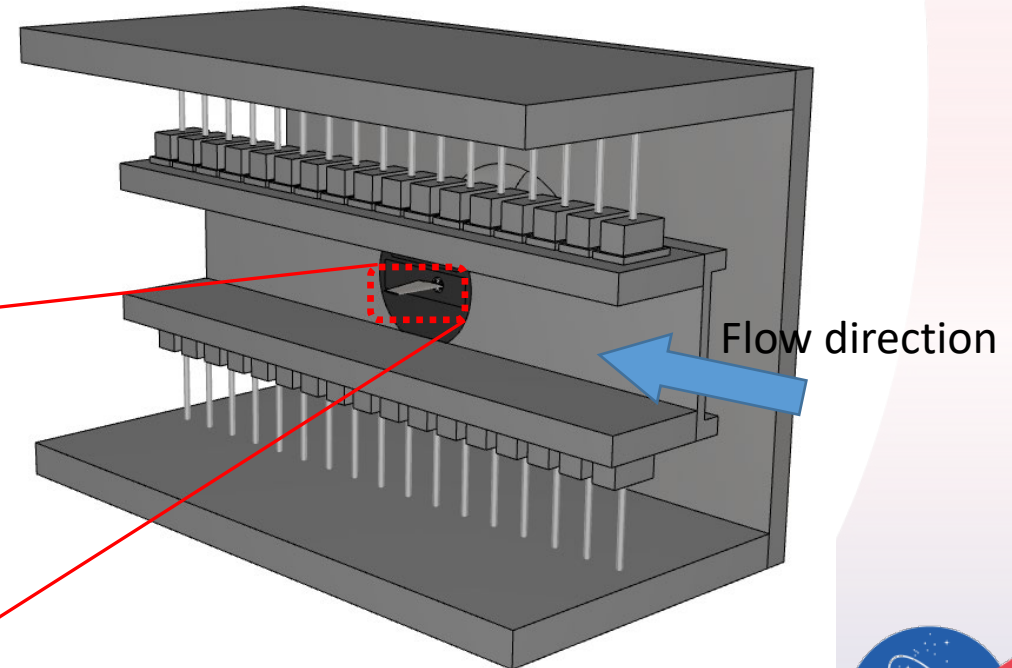
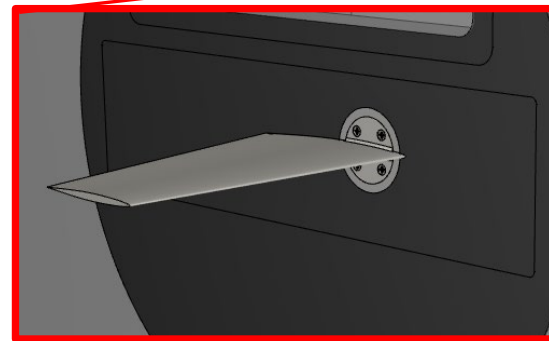
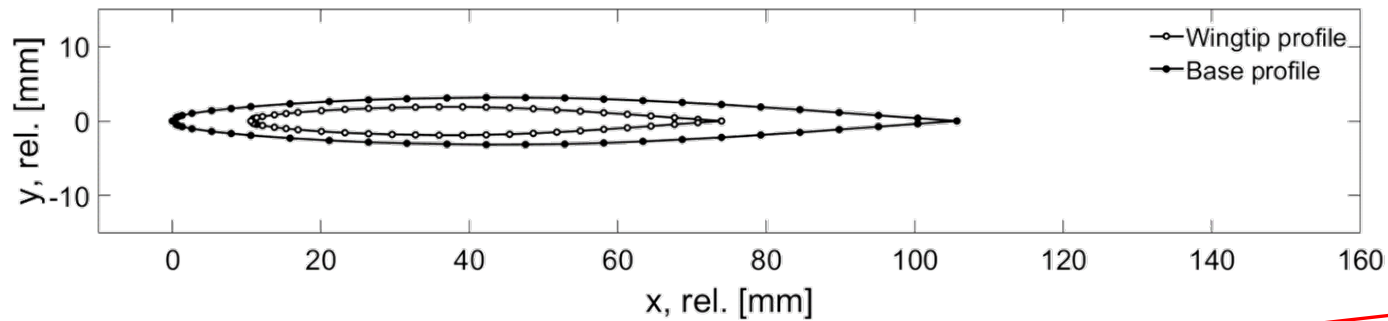
# Experimental Setup, Phase 2

---

# Experimental Setup, Phase 2

**Phase 2 Studies** – Assess particles for sensitivity to flow separation under high-lift tunnel operating conditions and model geometry

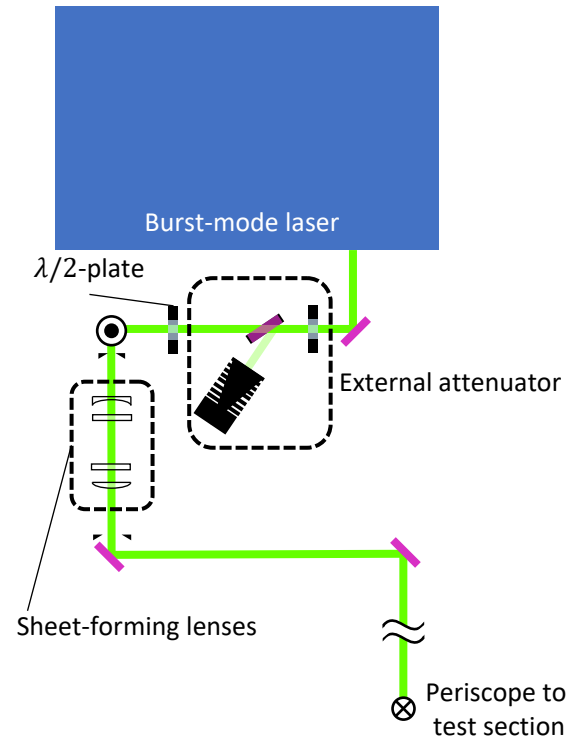
- Low-Mach-#, High- $\alpha$
- Stand-in for conditions experienced in upcoming (possibly ongoing CRM-HL experiments in the NTF)
- Semi-span airfoil used in the studies
  - NACA 65A006 airfoil



# Experimental Setup, Phase 2

## Laser and imaging systems

- Burst-mode laser

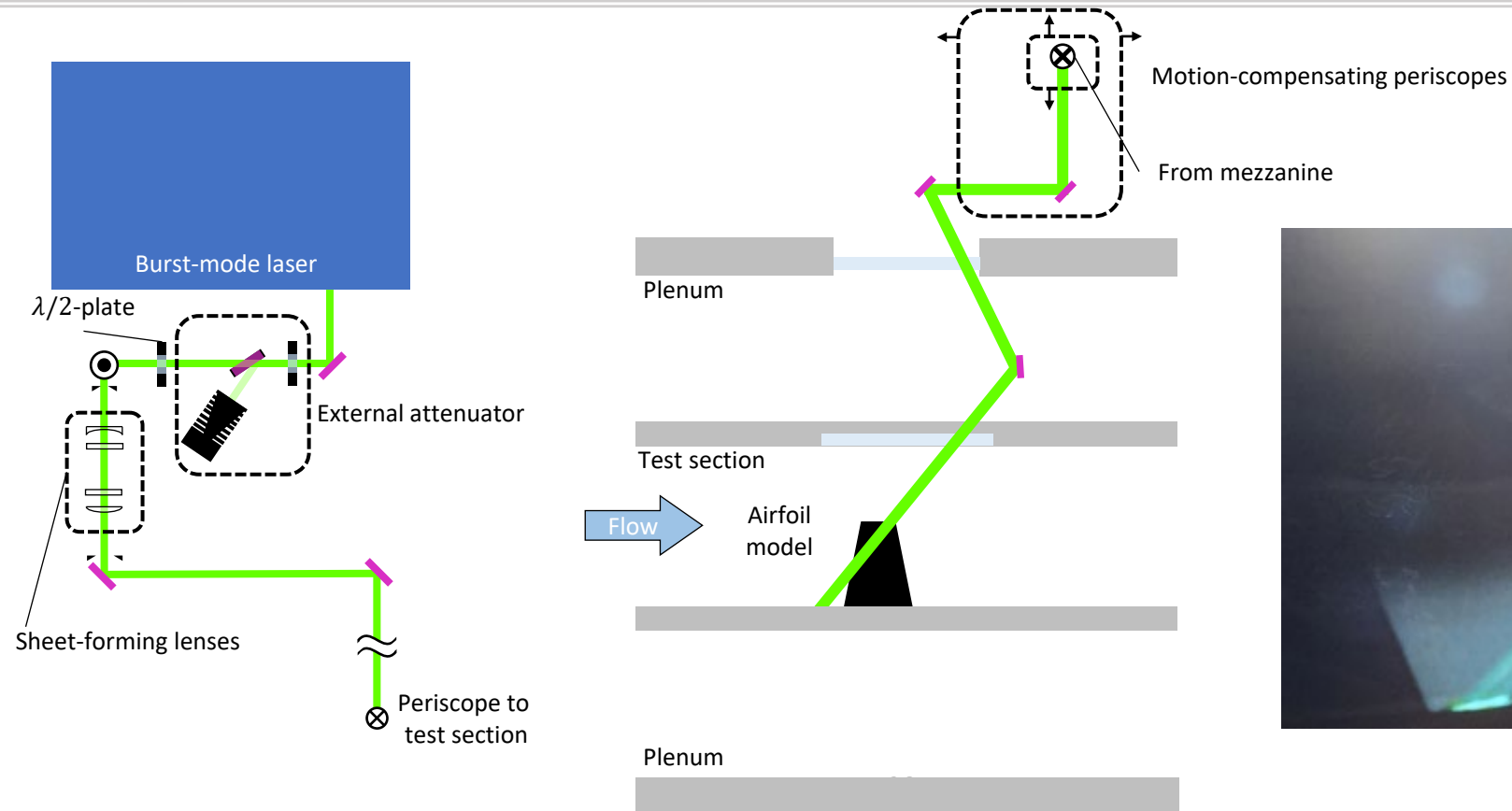


Center Wavelength	532.217 nm
Pulse Duration	20 ns
Repetition Rate	100 kHz
Operating Mode	Single pulse
Burst Duration	10 ms
Burst Period	12 s

# Experimental Setup, Phase 2

## Laser and imaging systems

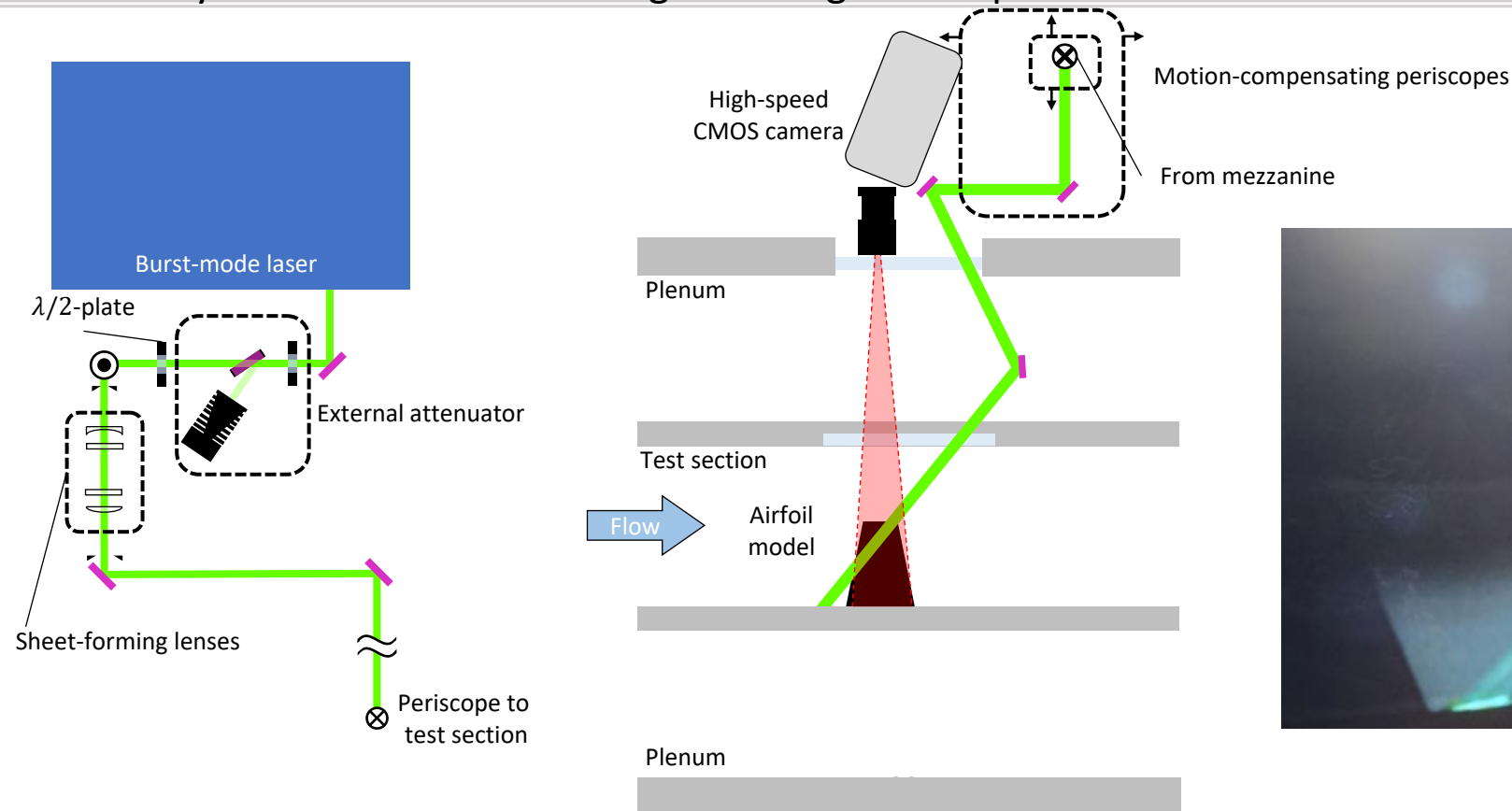
- Burst-mode laser
- Beam directed through an external attenuator and sheet-forming optics on upper mezzanine
- Laser sheet transmitted to test section area and through plenum and test section via numerous mirrors
- Sheet passed over model at an oblique angle ( $\sim 55^\circ$  WRT streamwise direction)
  - Final dimensions  $\sim 40$  mm (height) x 5 mm (thickness)



# Experimental Setup, Phase 2

## Laser and imaging systems

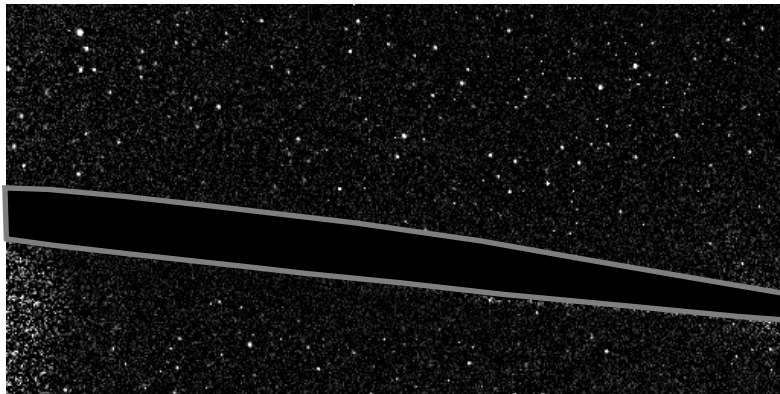
- Burst-mode laser
- Beam directed through an external attenuator and sheet-forming optics on upper mezzanine
- Laser sheet transmitted to test section area and through plenum and test section via numerous mirrors
- Sheet passed over model at an oblique angle ( $\sim 55^\circ$  WRT streamwise direction)
  - Final dimensions  $\sim 40$  mm (height) x 5 mm (thickness)
- High-speed CMOS synced with laser and imaged through outer pressure-shell window and internal slot window



# Experimental Setup, Phase 2

## Data Sample

- Because the camera is aligned (orthogonal) to the streamwise direction measurement, measurement is principally detecting streamwise movement of the particles (through the thickness of the laser sheet)
- Particle tracking velocimetry (PTV) performed on data after preprocessing of images



Sample data (background subtracted)  
(Mach 0.25, AoA 8 deg)

Measurement plane not in  
streamwise direction



# Results, Phase 2

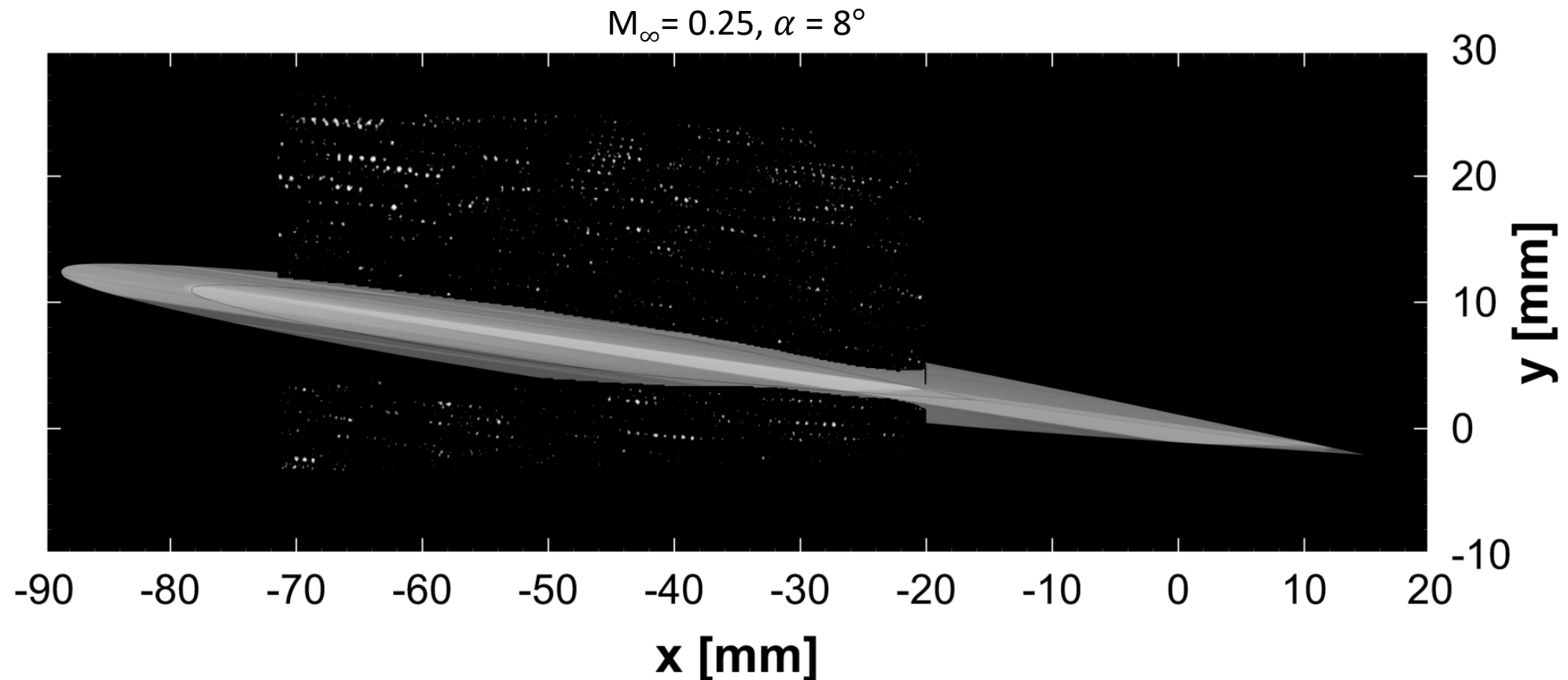
## Streak images

- Constructed from preprocessed data, allow the visualization of particle trajectories over time

# Results, Phase 2

## Streak images

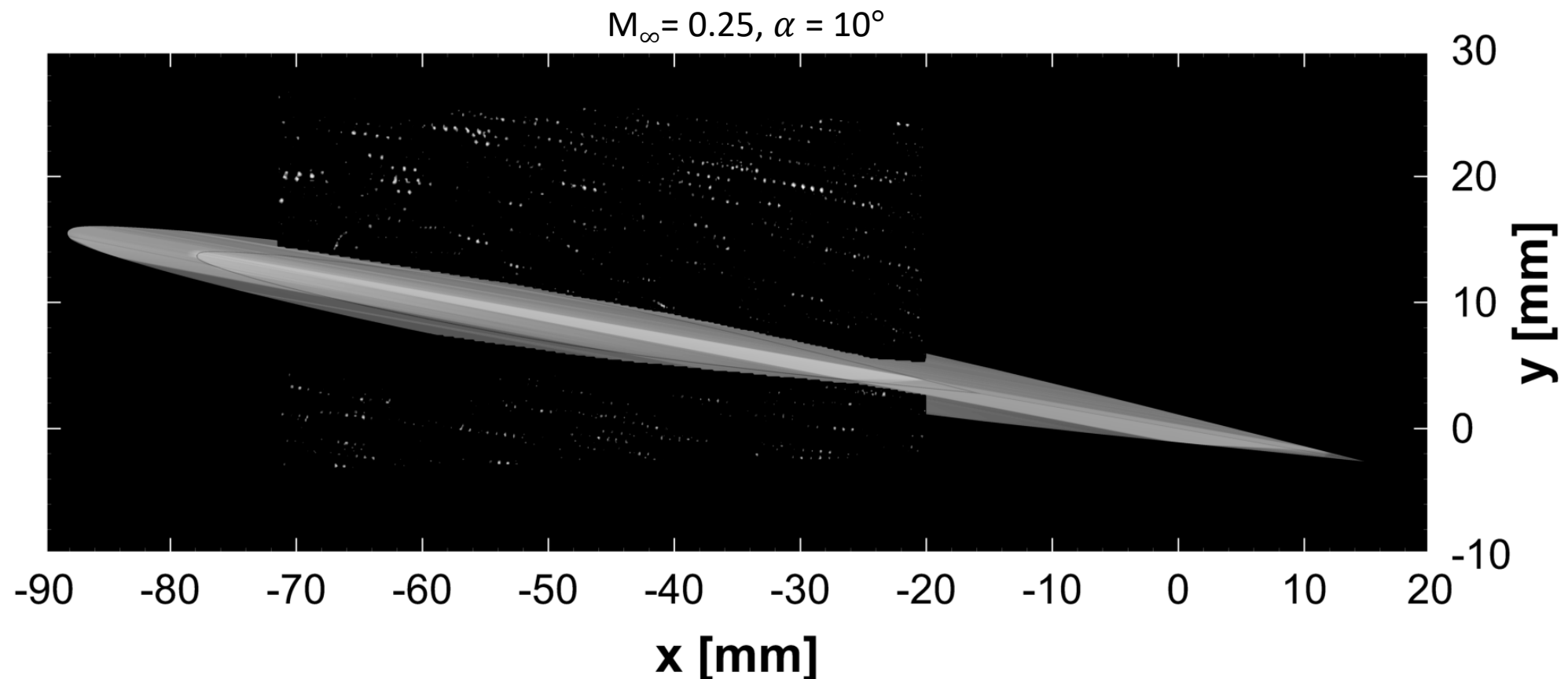
- Constructed from preprocessed data, allow the visualization of particle trajectories over time
- $\alpha = 8^\circ$  : Uniform tangential motion in areas above and below airfoil



# Results, Phase 2

## Streak images

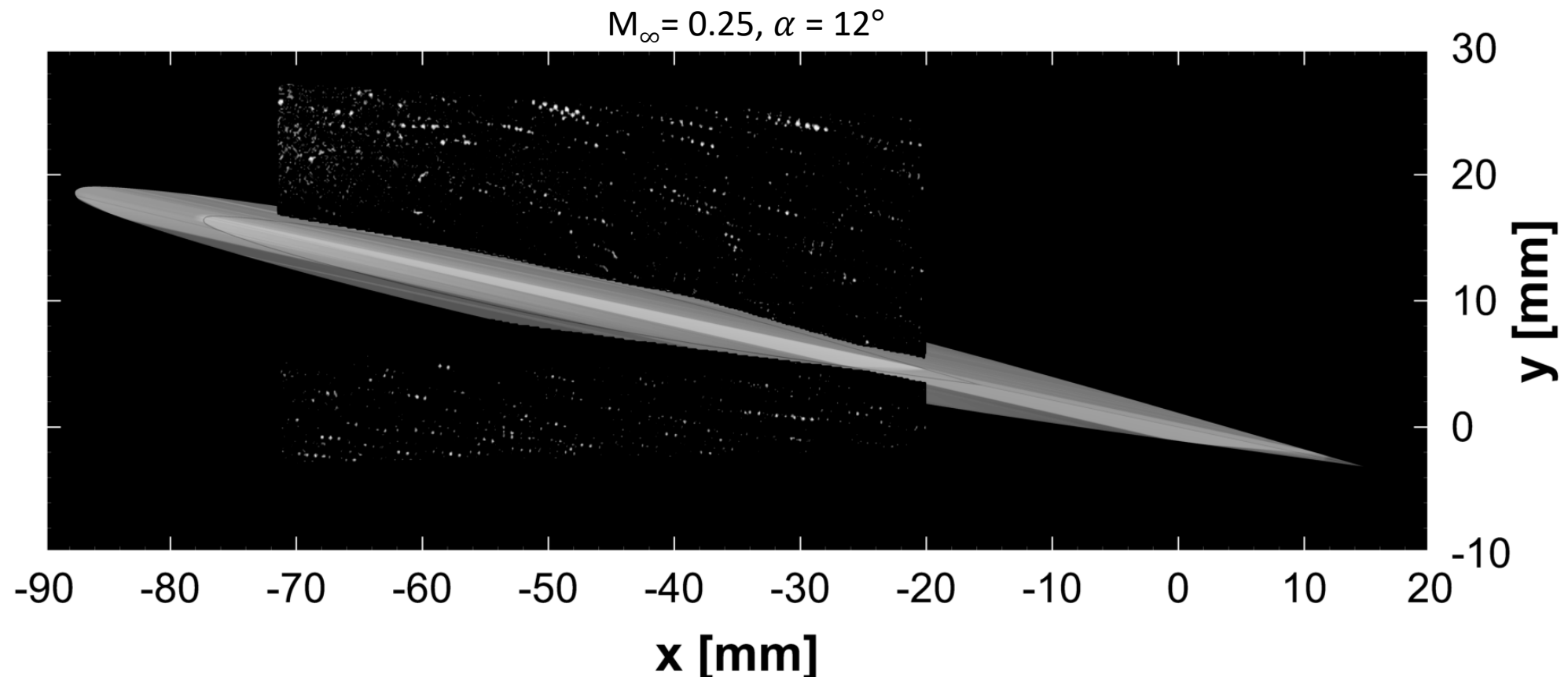
- Constructed from preprocessed data, allow the visualization of particle trajectories over time
- $\alpha = 8^\circ$  : Uniform tangential motion in areas above and below airfoil
- $\alpha = 10^\circ$ : Intermittent reversed and stagnant motion on top surface of airfoil (incipient separation)



# Results, Phase 2

## Streak images

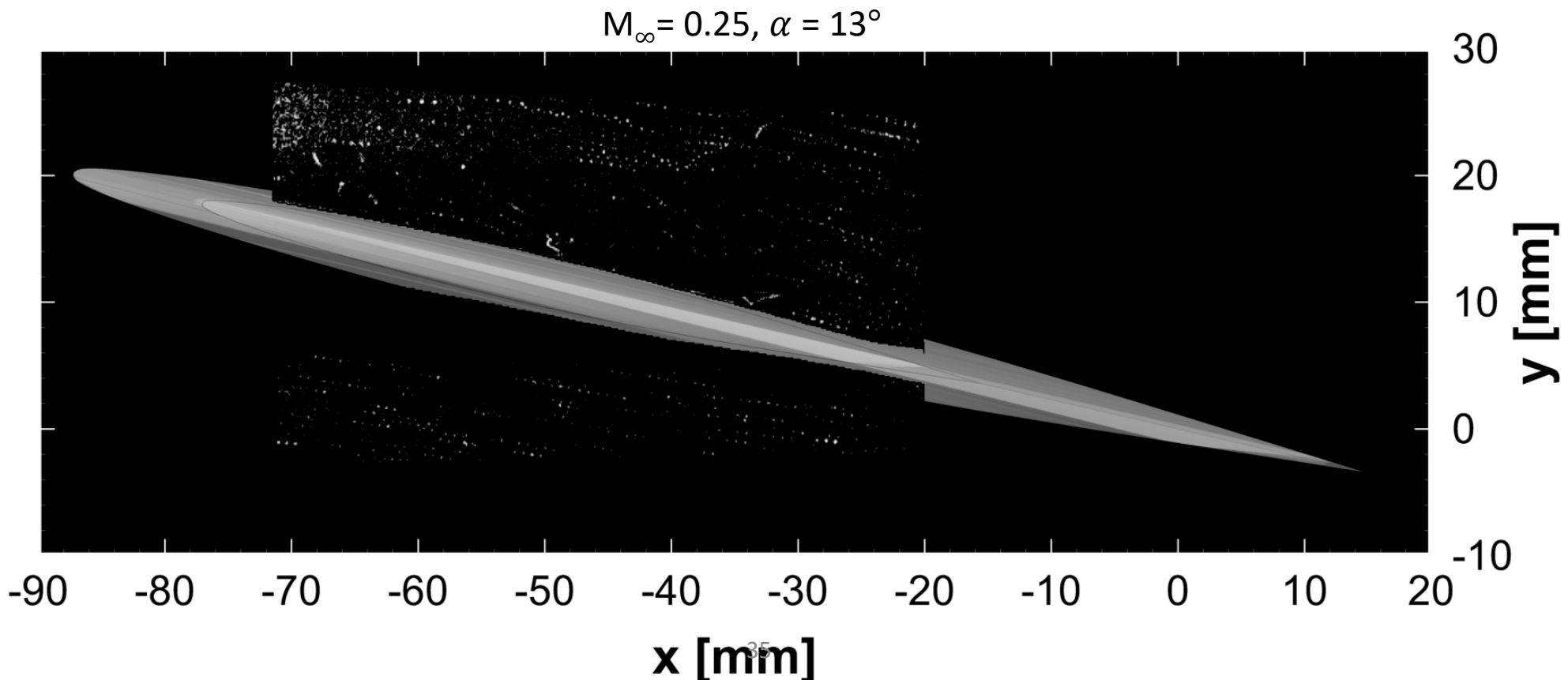
- Constructed from preprocessed data, allow the visualization of particle trajectories over time
- $\alpha = 8^\circ$  : Uniform tangential motion in areas above and below airfoil
- $\alpha = 10^\circ$  : Intermittent reversed and stagnant motion on top surface of airfoil (incipient separation)
- $\alpha = 12^\circ$  : Continuous region of reversed and stagnant flow on upper airfoil surface (complete separation)



# Results, Phase 2

## Streak images

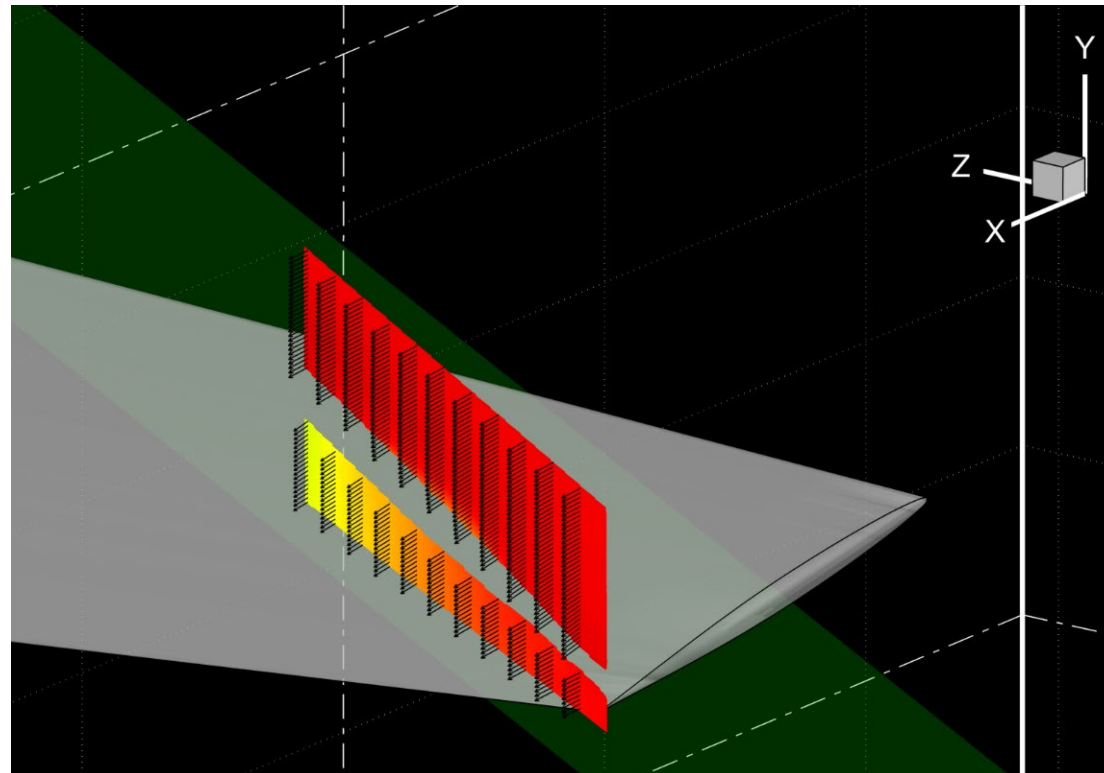
- Constructed from preprocessed data, allow the visualization of particle trajectories over time
- $\alpha = 8^\circ$  : Uniform tangential motion in areas above and below airfoil
- $\alpha = 10^\circ$  : Intermittent reversed and stagnant motion on top surface of airfoil (incipient separation)
- $\alpha = 12^\circ$  : Continuous region of reversed and stagnant flow on upper airfoil surface (complete separation)
- $\alpha = 13^\circ$  : Streamwise/spanwise expansion of separated region



# Results, Phase 2

Mean velocity fields

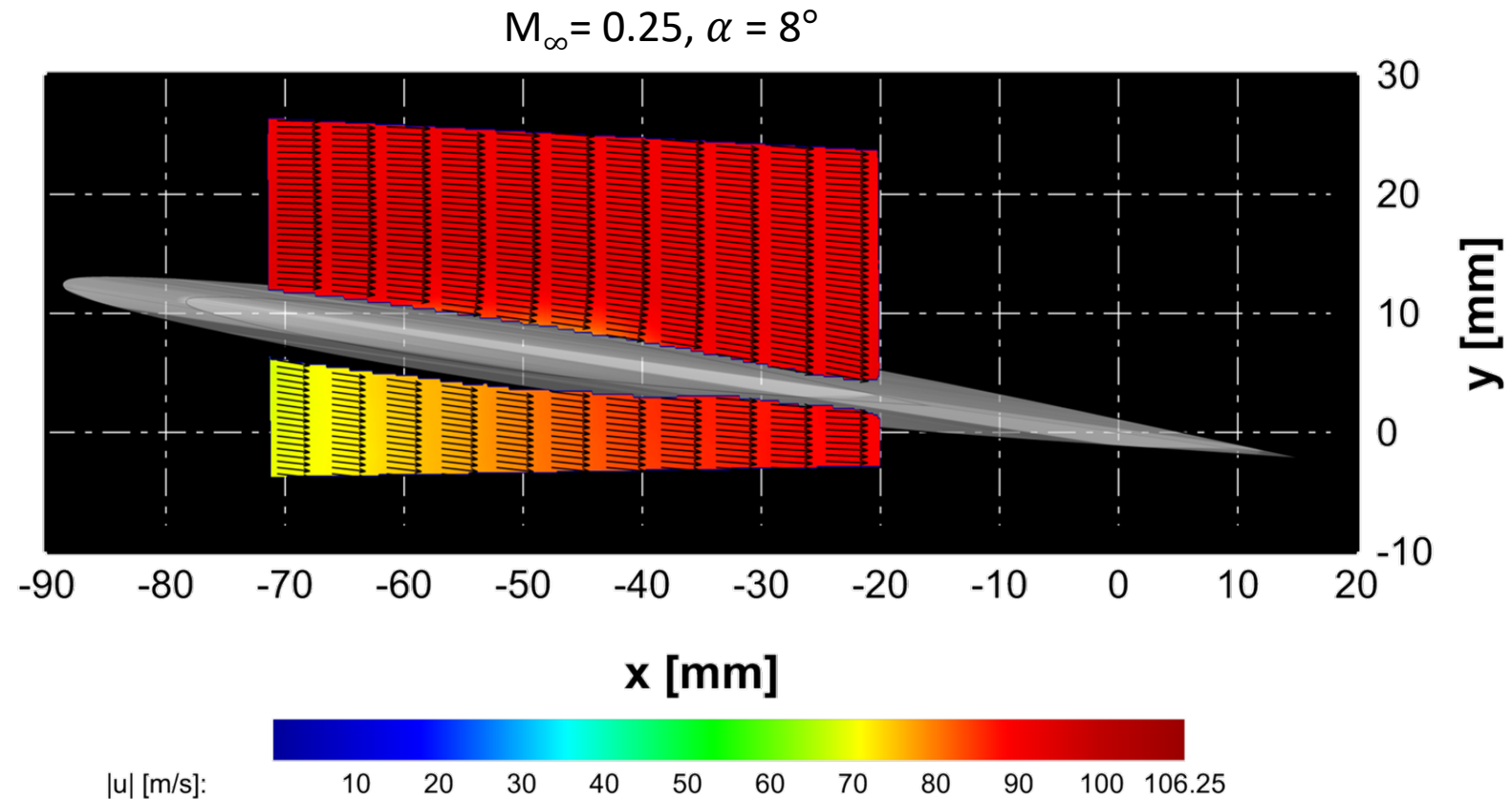
3D orientation of vectors



# Results, Phase 2

## Mean velocity fields

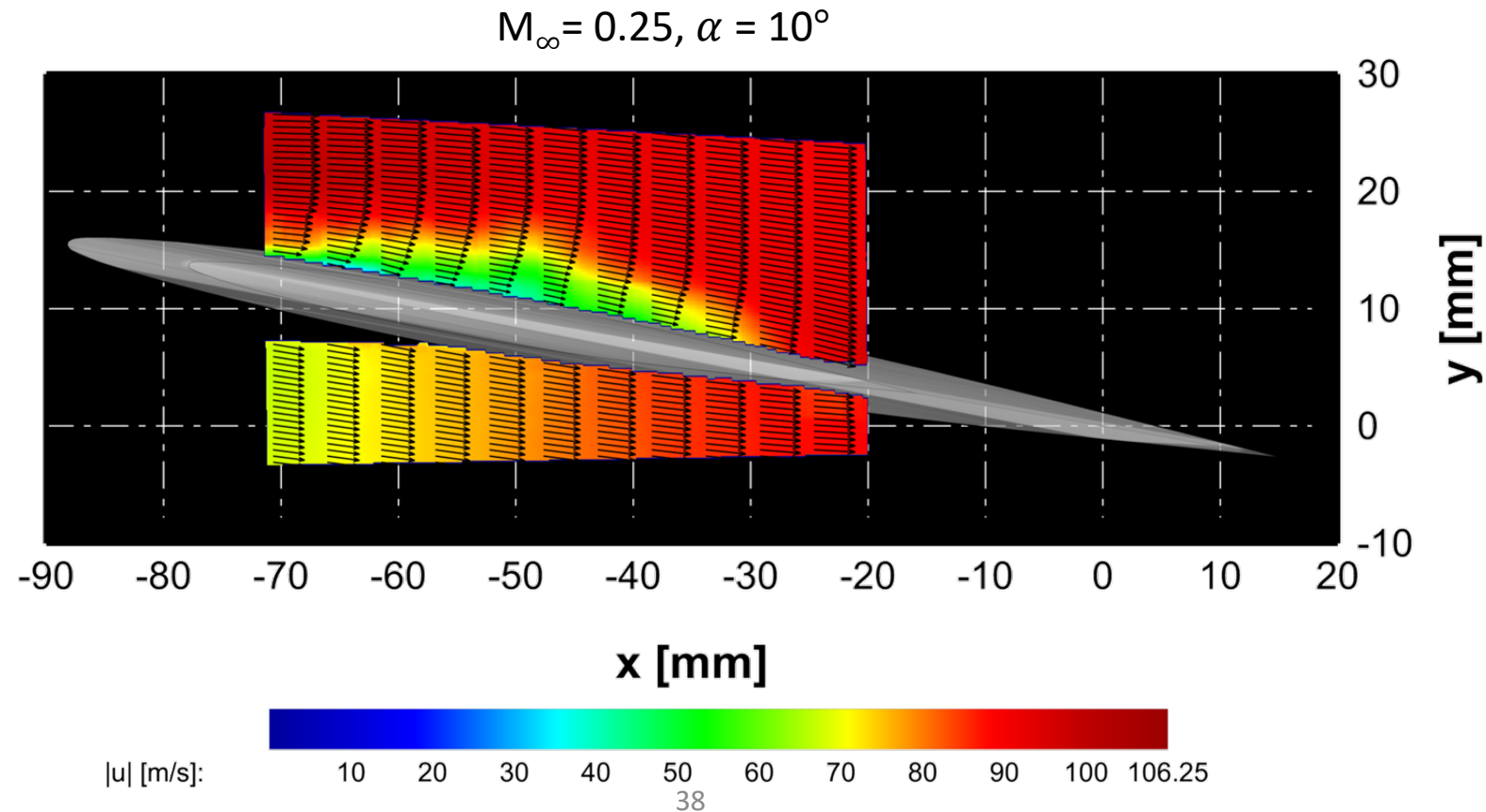
- Reflect general observations made in streak images
- $\alpha = 8^\circ$  : Flow is uniformly tangent to airfoil surface, obvious gradient in velocity on underside of airfoil



# Results, Phase 2

## Mean velocity fields

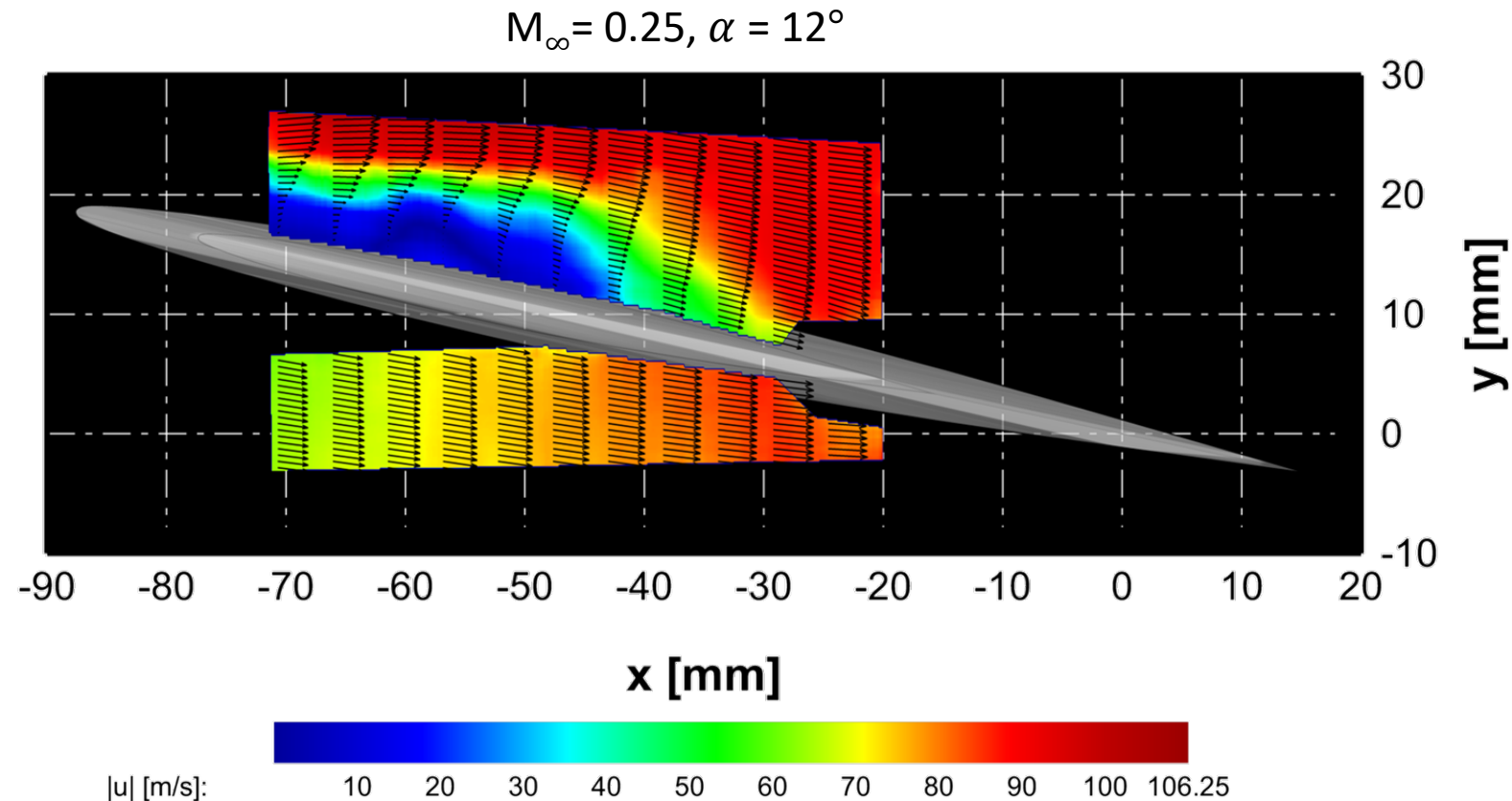
- Reflect general observations made in streak images
- $\alpha = 8^\circ$  : Flow is uniformly tangent to airfoil surface, obvious gradient in velocity on underside of airfoil
- $\alpha = 10^\circ$  : No mean reversed or stagnant flow observed on upper surface, region of decreased velocity (consistent with IS)



# Results, Phase 2

## Mean velocity fields

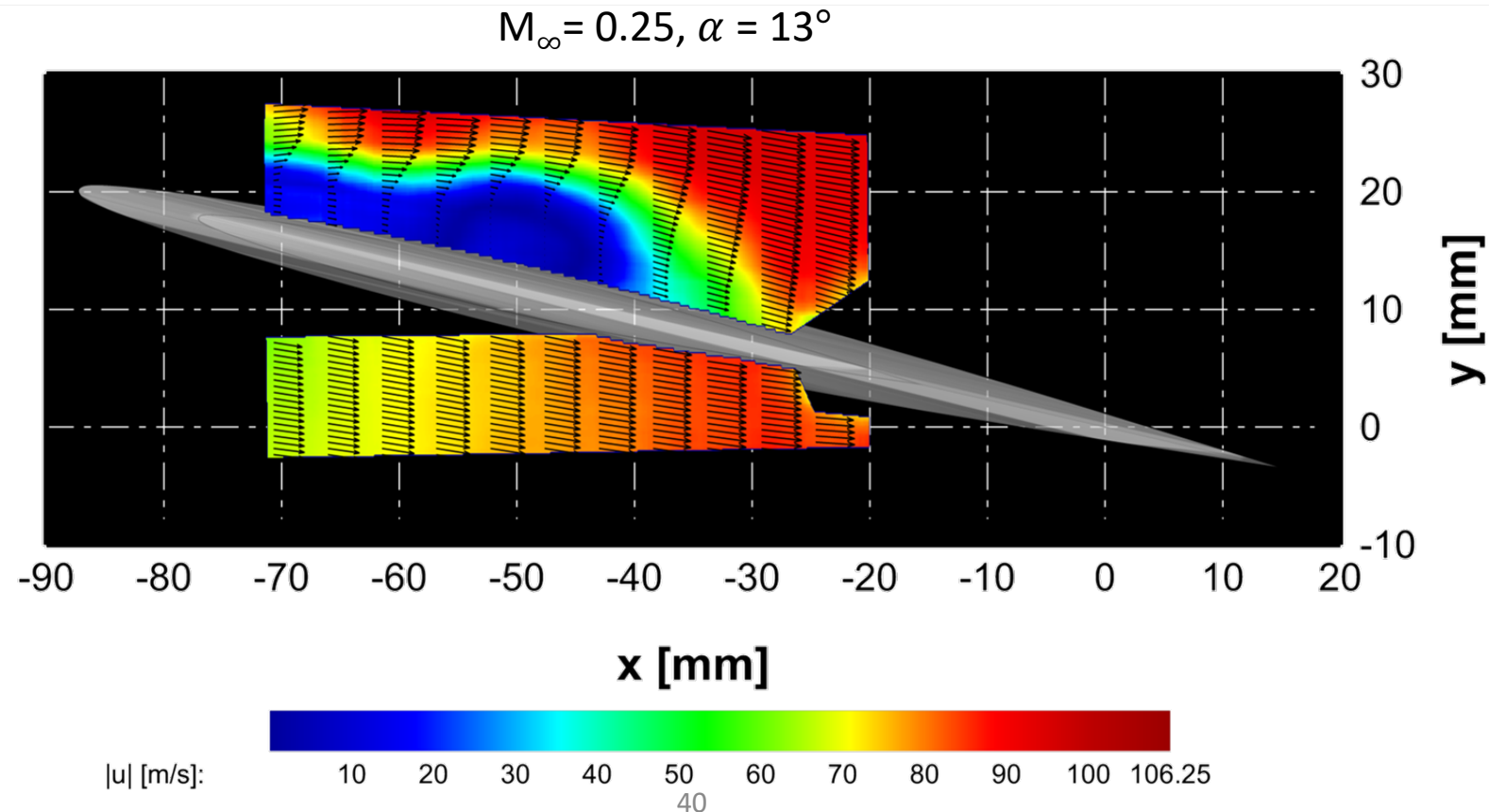
- Reflect general observations made in streak images
- $\alpha = 8^\circ$  : Flow is uniformly tangent to airfoil surface, obvious gradient in velocity on underside of airfoil
- $\alpha = 10^\circ$  : No mean reversed or stagnant flow observed on upper surface, region of decreased velocity (consistent with IS)
- $\alpha = 12^\circ$  : Large region of separated flow on upper surface, region appears to be stagnant (slightly reversed near surface)



# Results, Phase 2

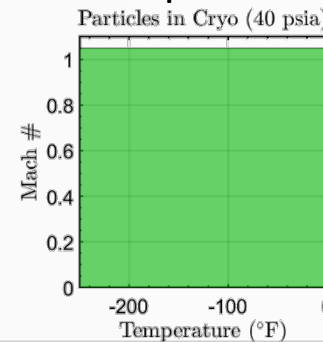
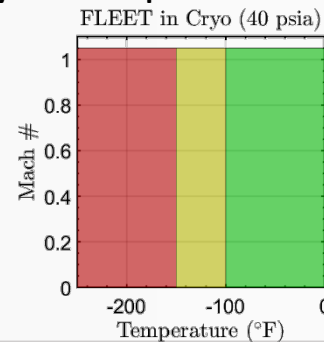
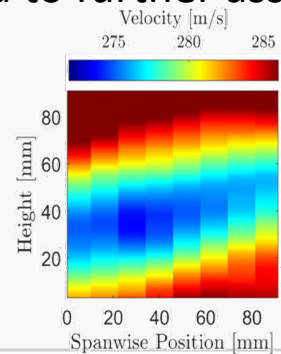
## Mean velocity fields

- Reflect general observations made in streak images
- $\alpha = 8^\circ$  : Flow is uniformly tangent to airfoil surface, obvious gradient in velocity on underside of airfoil
- $\alpha = 10^\circ$  : No mean reversed or stagnant flow observed on upper surface, region of decreased velocity (consistent with IS)
- $\alpha = 12^\circ$  : Large region of separated flow on upper surface, region appears to be stagnant (slightly reversed near surface)
- $\alpha = 13^\circ$  : Expansion of the separated region, region of stagnant flow expanded and shifted downstream/medial

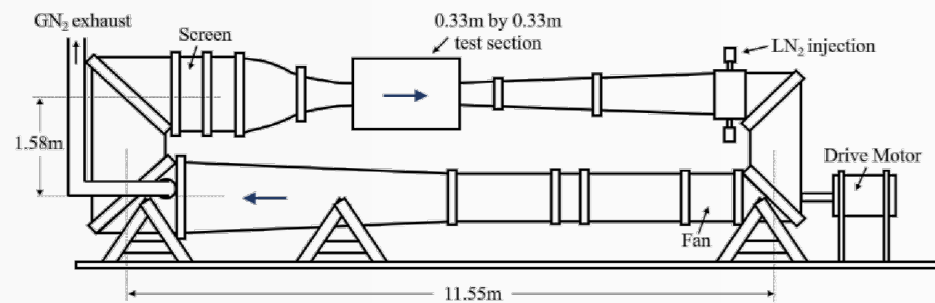


# Summary and Conclusions

- After years of modestly successful FLEET velocimetry measurements in NASA LaRC's TCT facilities, shifting toward particle-based measurements due to insufficient performance of FLEET over full operational envelope in the NTF
  - However it is beneficial to have two measurement techniques operating on different principles
- Naturally-occurring particles a likely candidate for their prevalence
- Need to further assess the aerodynamic performance of the particles



- Established and tested a framework in NASA LaRC's 0.3-m TCT for *in situ* particle response assessment
  - Use of a normal shockwave generated by an airfoil to induce velocity lag
  - *A posteriori* assessment of velocity distributions in separated flows

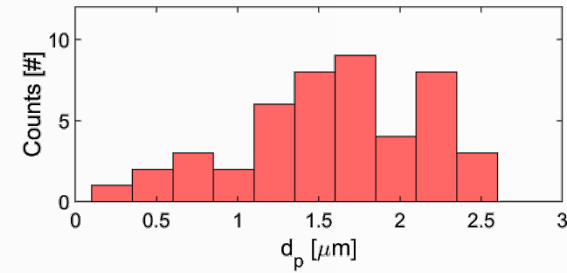
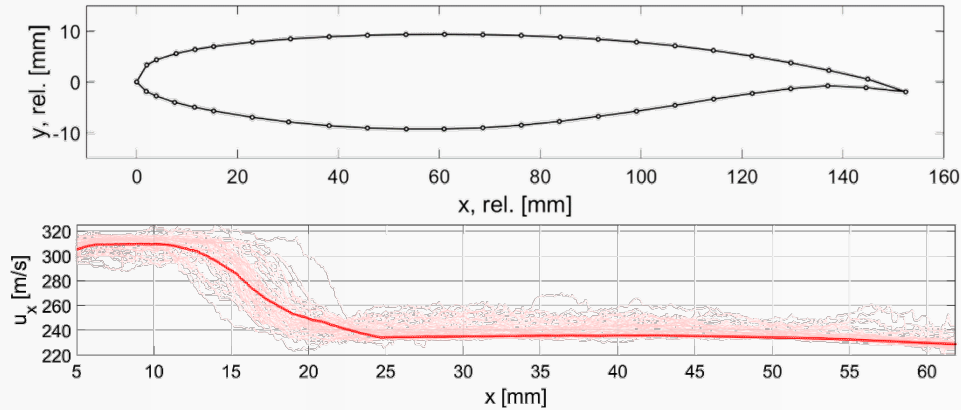


- Currently implementing PTV in the National Transonic Facility (NTF)

# Summary and Conclusions

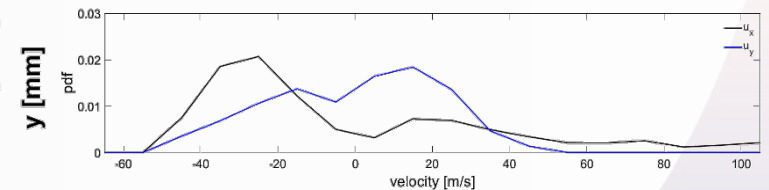
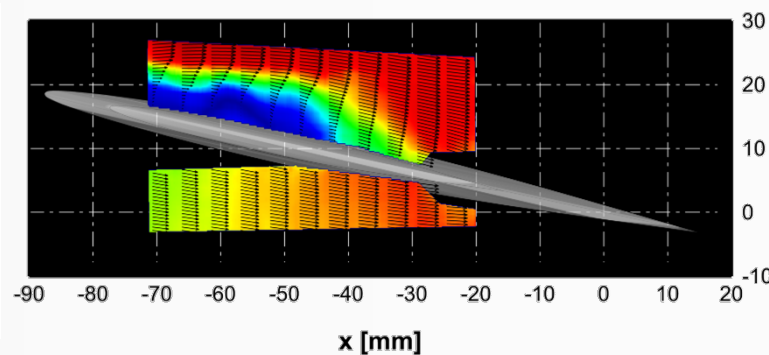
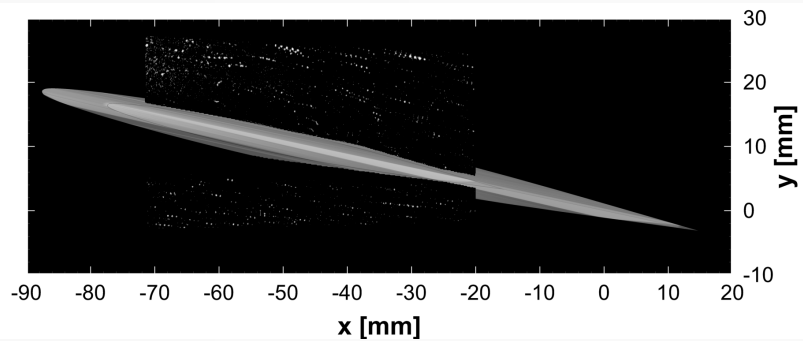
**Phase 1 Studies:** Performed a particle response assessment using a supercritical airfoil to generate a normal shockwave

- Found stable operating conditions using SAFS system
- Mean particle diameter found to lie between 1.6 and 1.9  $\mu\text{m}$  and ranged from 0.2 to 3.5  $\mu\text{m}$



**Phase 2 Studies:** Observed and measured particle behavior in representative high-lift conditions for sensitivity to separated flow

- Transition from fully attached to fully separated detected from 8° to 13° angle of attack sweep
- Velocity distribution within separated flow regions indicate a small fraction of particles (5-7 %) unresponsive to the separated regions



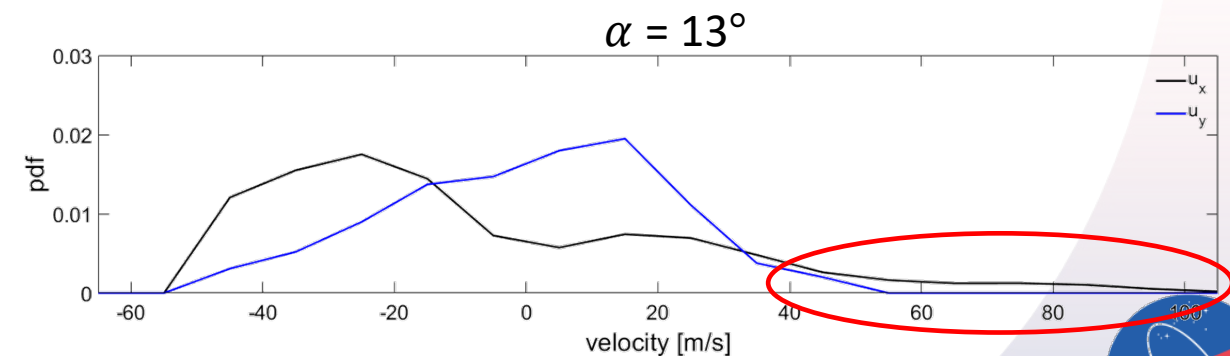
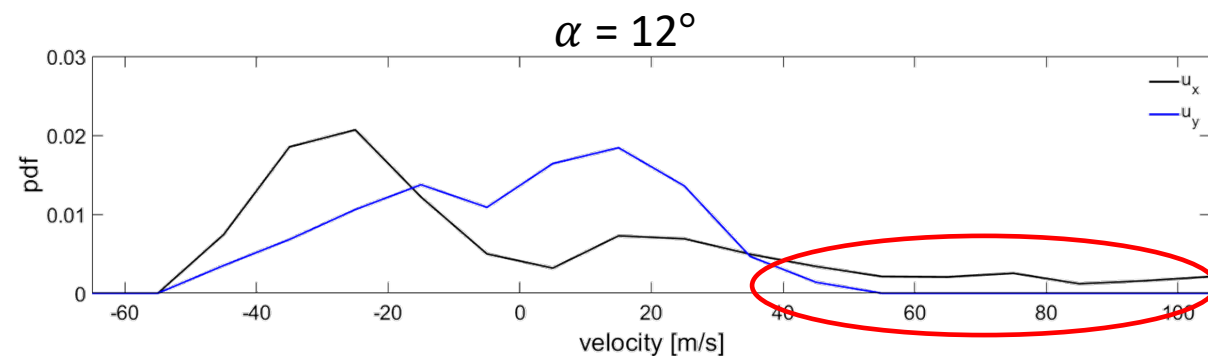
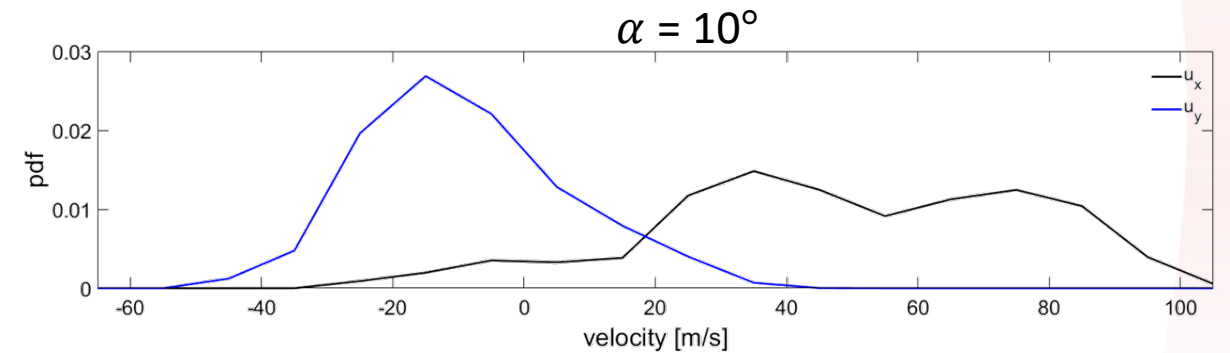
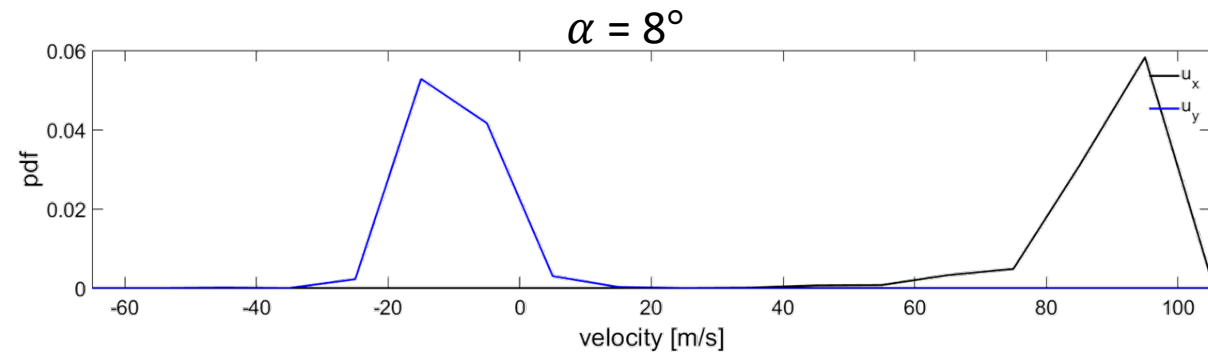
# Backup Charts

---

# Results, Phase 2

## Velocity distributions (probability density functions)

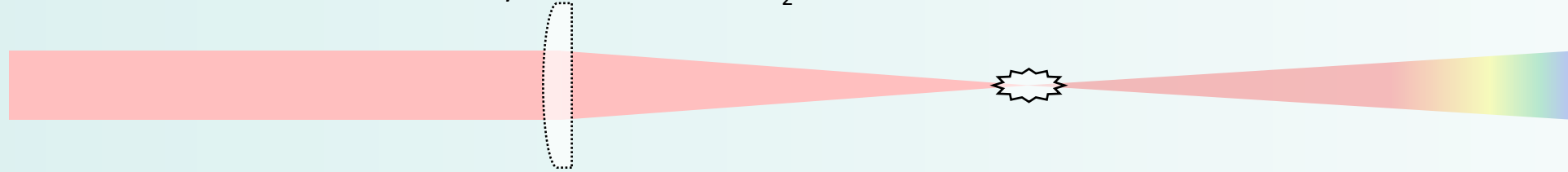
- Sampled in low velocity/separated flow region
- At lowest angle of attack ( $8^\circ$ ), see focal clusters consistent with uniform tangential motion seen in the mean velocity field
- For all other cases, see much larger variance in the measured velocities (streamwise particularly) with a shift to lower and negative velocities at the highest angles of attack
- **Long tails** on the streamwise velocity distributions suggests larger particles unable to track with separation (5-7% total probability)



# Background and motivation

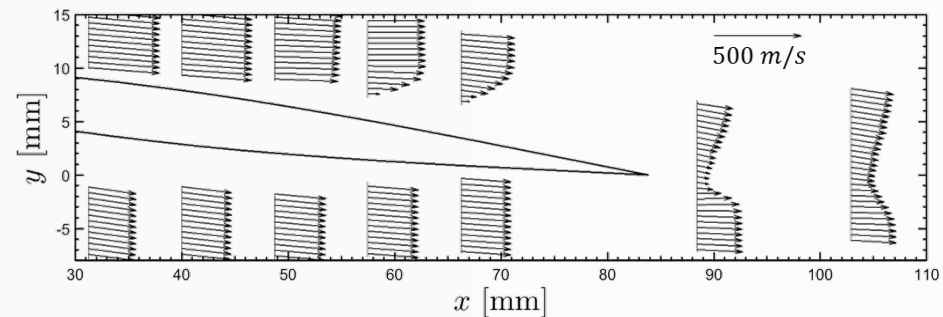
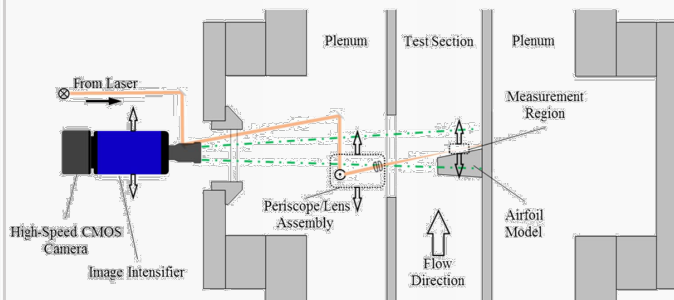
Successfully implemented a velocimetry system in NASA LaRCs TCT facilities (NTF, 0.3-m TCT) utilizing FLEET (Femtosecond Laser Electronic Excitation Tagging) velocimetry (Princeton)

- Unseeded optical velocimetry technique
- Femtosecond laser focused to dissociate/ionize molecular N<sub>2</sub>



## 0.3-m TCT – Transonic Airfoil (2016)

- Measured 2-component velocity profiles around a transonic airfoil model



AIAA JOURNAL  
Vol. 55, No. 12, December 2017

**Unseeded Velocity Measurements Around a Transonic Airfoil Using Femtosecond Laser Tagging**

Ross A. Burns\* and Paul M. Danehy<sup>†</sup>  
NASA Langley Research Center, Hampton, Virginia 23681  
DOI: 10.2514/1.056154

Femtosecond laser electronic excitation tagging velocimetry was used to study the flowfield around a symmetric, transonic airfoil in the NASA Langley Research Center's 0.3 m transonic cryogenic tunnel facility. A nominal Mach number of 0.85 was investigated with a total pressure of 125 kPa and a total temperature of 280 K. Two components of velocity were measured along vertical profiles at different locations above, below, and aft of the airfoil at angles of attack of 0 and 7 deg. Velocity profiles within the wake showed sufficient accuracy, precision, and sensitivity to resolve both the mean and fluctuating velocities and general flow physics, such as shear-layer growth. Evidence of flow separation was found at high angles of attack. Velocity measurements were assessed for their accuracy, precision, dynamic range, spatial resolution, and overall measurement uncertainty as they relate to the present experiments. Measurement precisions as low as 1 m/s were observed, whereas the velocity dynamic range was found to be nearly a factor of 500. The spatial resolution of between 1 and 5 mm was found to be primarily limited by the femtosecond laser electronic excitation tagging spot size and advection of the flow. Overall measurement uncertainties ranged from 3 to 4%.

**Nomenclature**

*a* = acceleration, m/s<sup>2</sup>  
*f* = lens effective focal length, mm  
*s* = generic displacement, m  
*t* = time, s

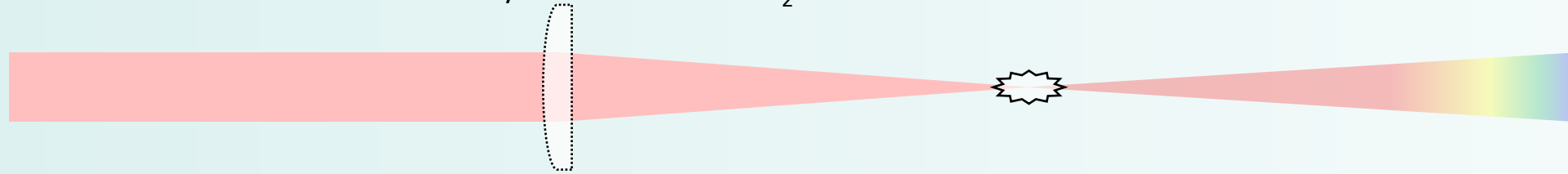
facility flow circuits, which (upon evaporation) reduces the operating temperature and simultaneously increases the flow density and decreases the viscosity [1–3]. Although this mode of operating is advantageous for simulating aerodynamic effects, it necessitates a rugged construction to accommodate the high pressures and thermal

Burns, RA and Danehy, PM, "Unseeded Velocity Measurements Around a Transonic Airfoil Using Femtosecond Laser Tagging,"  
AIAA Journal 2017

# Background and motivation

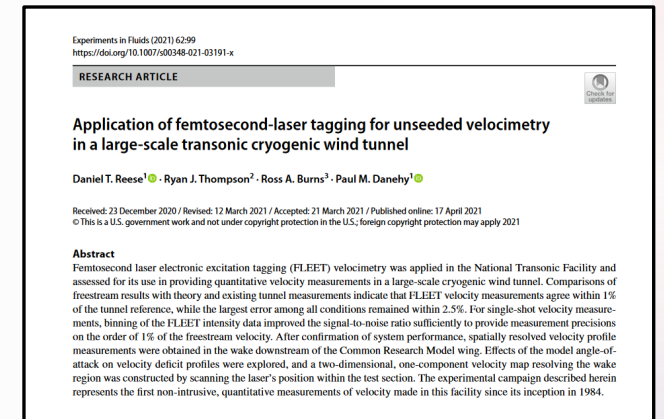
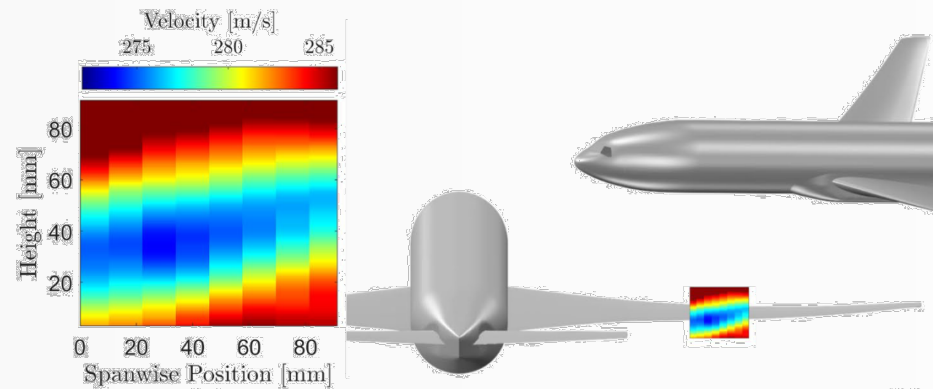
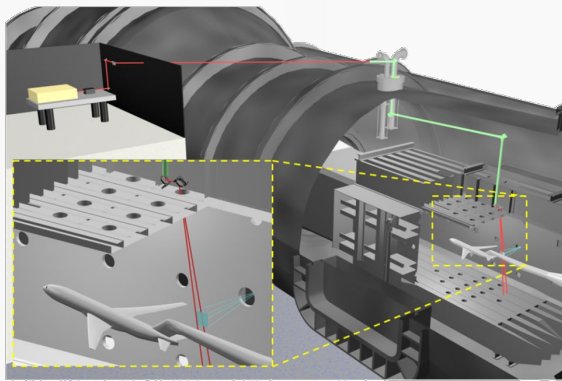
Successfully implemented a velocimetry system in NASA LaRCs TCT facilities (NTF, 0.3-m TCT) utilizing FLEET (Femtosecond Laser Electronic Excitation Tagging) velocimetry (Princeton)

- Unseeded optical velocimetry technique
- Femtosecond laser focused to dissociate/ionize molecular  $N_2$



## NTF – CRM Wake Velocity (2018)

- Measured two-dimensional velocity field in wake of the common research model in the NTF



Reese, DT, Thompson, RJ, Burns, RA, and Danehy, PM, "Application of femtosecond-laser tagging for unseeded velocimetry in a large-scale transonic cryogenic wind tunnel," Experiments in Fluids 2021